# DETERMINATION OF *IN VITRO* AND *IN SILICO* INDEXES FOR THE MODELLING OF BLOOD-BRAIN BARRIER PARTITIONING OF DRUGS VIA MICELLAR AND IMMOBILIZED ARTIFICIAL MEMBRANE LIQUID CHROMATOGRAPHY.

Giacomo Russo[1,2], Lucia Grumetto[2], Roman Szucs[3], Francesco Barbato[2], Frederic Lynen[1]*.

*corresponding author

1. Separation Science Group, Department of Organic and Macromolecular Chemistry, Ghent University, Krijgslaan 281, S4-bis, B-9000 Gent, Belgium

2. Dipartimento di Farmacia, Università degli Studi di Napoli Federico II, Via D. Montesano, 49 I-80131 Naples, Italy

3. Pfizer Global R&D, Sandwich CT13 9NJ, Kent, United Kingdom

# DETERMINATION OF *IN VITRO* AND *IN SILICO* INDEXES FOR THE MODELLING OF BLOOD-BRAIN BARRIER PARTITIONING OF DRUGS VIA MICELLAR AND IMMOBILIZED ARTIFICIAL MEMBRANE LIQUID CHROMATOGRAPHY.


## ABSTRACT

In the present work, 79 structurally unrelated analytes were taken into account and their chromatographic retention coefficients, measured by Immobilized Artificial Membrane Liquid Chromatography (IAM-LC), and by Micellar Liquid Chromatography (MLC) employing sodium dodecyl sulfate (SDS) as surfactant, were determined. Such indexes, along with topological and physico-chemical parameters calculated *in silico,* were subsequently used for the development of Blood-Brain Barrier passage-predictive statistical models using partial least square (PLS) regression.. Highly significant relationships were observed either using IAM ($r^2$ ($n$-1) = 0.78) or MLC ($r^2$ ($n$-1) = 0.83) derived indexes along with *in silico* descriptors. This hybrid approach proved fast and effective in the development of highly predictive BBB passage oriented models and, therefore, it can be of interest for pharmaceutical industries as a high-throughput BBB penetration oriented screening method. Finally, it shed new light into the molecular mechanism involved in the BBB uptake of therapeutics.



*Keywords*: Immobilized Artificial Membrane; Micellar Liquid Chromatography; Blood-Brain Barrier passage; Quantitative structure–activity relationships.

## 1.0 INTRODUCTION

Pharmaceutical drug development is still a highly inefficient process: over one third of the failures in drug candidate development is estimated to occur due to unsatisfactory pharmacokinetic properties[1], mainly regarding absorption, metabolism and toxicity and the attrition rates for Central Nervous System (CNS) active drugs are even higher[2]. In fact, before reaching the blood circulation, a drug diffuses through the biological barriers separating the circulating blood from the interstitial fluid that surrounds the tissues. For orally administered drugs, this barrier is the intestinal epithelium whereas the passage of drugs designed to act at the CNS level is further regulated by the Blood-Brain Barrier (BBB). The BBB is one of the most complex and extensively studied biological barriers, and its function is to preserve mammalian brain integrity against possible injurious substances. It is made of endothelial cells, narrowly adherent one to the other to form tight junctions, restricting the passage of solutes[3,4]. Indeed, drug transport is strongly limited by this peculiar biological structure to pure passive transcellular diffusion. In fact, the paracellular route, i.e. the passage of actives through the gaps between each endothelial cell, is completely hindered. Apart from active transport mechanisms, whose occurrence is difficult to predict on a solely chemical structure basis, drugs can therefore cross the BBB only by the passive transcellular route. Plenty of *in vivo*, *ex vivo*, and *in vitro* methods are available for measuring BBB partitioning of analytes. Historically, one of the most used and reputed method is the determination of log BB values[5]. Log BB is defined as:

$$\log BB = \log \frac{C_{Brain}}{C_{Blood}}$$

in which $C_{Brain}$ is the concentration that the analyte realizes in the brain tissues, and $C_{Blood}$ is the concentration that it realizes in the blood. However, this method involves the use of animal models,

usually rodents, and does not provide any mechanistic information about the nature of the passage; furthermore, the method is time-consuming and potential source of ethical issues.

Methods based on the employment of cultured cell lines can also be effective; however, astrocytes cell cultures are often difficult to grow and recreating an *in vitro* environment similar to the *in vivo* BBB can be challenging even for the most experienced scientists. Caco-2 model based methods may also be an alternative; however, apart from the structural dissimilarities with the other cell cultures[6], they are difficult to standardize, complicating comparisons of data determined in different laboratories.

*In silico* methods, generally based on the calculation of physico-chemical parameters, yield various advantages. They are much faster to perform, allowing the screening of large libraries of compounds (even solutes not yet synthesized); in addition, they can assist in the elucidation of the molecular mechanisms involved in membrane permeation. However, they also suffer from several limitations including the aspect that they are unable to take into account all phenomena actually occurring *in vivo*[7] .

*In vitro* methods based on the use of biomimetic stationary phases coupled with high performance liquid chromatography (HPLC) have been used to surrogate BBB permeation data[8,9]. The main advantages are that they are much more reproducible and easier to perform and, albeit conceptually simple, they can be incidentally able to provide an in-depth understanding of the mechanisms involved in membrane barrier passage. Such biomimetic stationary phases include, for instance, Immobilized Artificial Membranes (IAM). IAM stationary phases are based on analogues of phosphatidylcholine, which is the major component of biological membranes, and chromatographic retention coefficients of the analytes on such stationary phases are assumed as direct measures of their phospholipophilicity[10], i.e. their affinity for phospholipids. Such measures have been proven to be able to mirror various phenomena underlying membrane barrier passage[8,11–13]. In addition, other chromatographic indexes, whose drug BBB-penetration predictivity has been demonstrated[14–16], include those achieved by Micellar Liquid Chromatography (MLC) technique. This technique is

84 based on the addition of surfactants to an aqueous mobile phase at concentrations higher than their
85 critical micelle concentrations (CMC)[17] resulting in the formation of micelles acting as a partition
86 phase. Both IAM and MLC chromatographic indexes, mainly if combined with *in silico* calculated
87 descriptors, have demonstrated effectiveness in the prediction of BBB drug penetration[16]. However,
88 the methods proposed are still too time-consuming to meet the demands of pharmaceutical
89 companies and their suitability should be confirmed on larger set of analytes.
90 The aim of the present work has been the development of drug BBB penetration oriented statistical
91 models based on analytical indexes, achieved on biomimetic conditions by medium/high-
92 throughput methods, along with *in silico* calculated descriptors. To the best of our knowledge, this
93 is the study based on the highest number of compounds among those employing IAM and MLC
94 data to predict drug pharmacokinetic properties.
95 Therefore, particular attention is set on:
96 *i*) the setup of medium/high-throughput methods for the achievement of both IAM and MLC
97 indexes;
98 *ii*) the validation of such parameters by developing statistical models for the prediction of BBB
99 penetration (log BB) by using the chromatographic indexes along with *in silico* calculated
100 descriptors;
101 *iii*) the elucidation of the molecular mechanism involved in BBB passive diffusion of drugs;
102 *iv*) the possibility of taking into account, by molecular docking studies, the occurrence of active
103 efflux mechanisms.
104 In the present work, 79 structurally unrelated analytes have been taken into account and their
105 chromatographic retention coefficients, measured by high-throughput IAM-LC and MLC methods,
106 the latter employing sodium dodecyl sulfate (SDS) as surfactant, were determined. Such indexes
107 have subsequently been used for the development of BBB-passage predictive statistical models
108 using partial least squares (PLS) automatic regression along with physico-chemical parameters,
109 calculated *in silico*. Such hybrid approach was aimed at combining the speediness in the

110 achievement of computational chemistry derived topological and physico-chemical parameters with
111 the improved predictivity of the *in vitro* methods.
112
113 **2.0 RESULTS AND DISCUSSION**

114 The IAM-LC and MLC chromatographic retention coefficients, as well as the pKa, log BB values,
115 UV wavelengths of the experimental determinations and suppliers, are presented in Table 1. In
116 MLC, the highest retained compound (triprolidine) eluted within 33.0 minutes, whereas in IAM-LC
117 the maximum run time was 37.0 minutes (fluphenazine). However, by performing either the MLC
118 or the IAM-LC analytical methods, 85% of the compounds of the dataset eluted within 15.0 minutes
119 and a preliminary estimate, as an order of magnitude, of the retention times expected can be easily
120 performed based on the calculation of log $D^{7.4}$ values of each compound present in the dataset. Two
121 chromatographic runs for each technique are reported in Figure 1 (MLC) and Figure 2 (IAM-LC).
122 The log BB values span a very large range (from -2.00 to +1.51) as the analytes to be included in
123 the dataset were selected to include both CNS inactive (e.g. norfloxacin, nitrofurantoin) and CNS
124 active (e.g. fluphenazine, desipramine) drugs. The P-gp affinities, expressed in $kcal \cdot mol^{-1}$, of the
125 drugs considered are listed in Table 2A and Table 2B. They were incorporated in each of the
126 following steps to model even the BBB passage of analytes undergoing P-gp effux mechanisms.
127

**Figure 1.** MLC chromatograms achieved for the analytes A) Imipramine (50 μg $mL^{-1}$ in methanol) and B) Ethylbenzene (50 μg $mL^{-1}$ in methanol) employing a mobile phase consisting of an aqueous solution of 0.05 $mol \cdot L^{-1}$ sodium dodecyl sulfate. The detailed experimental conditions are reported in paragraph 4.0.

A

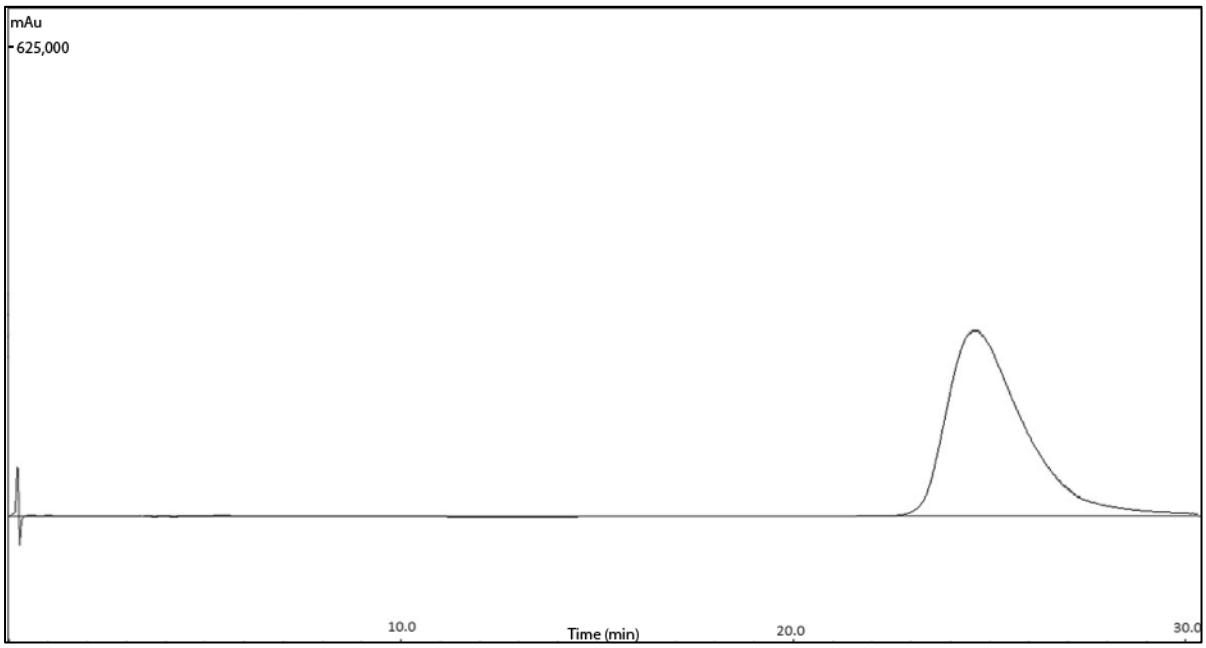


B

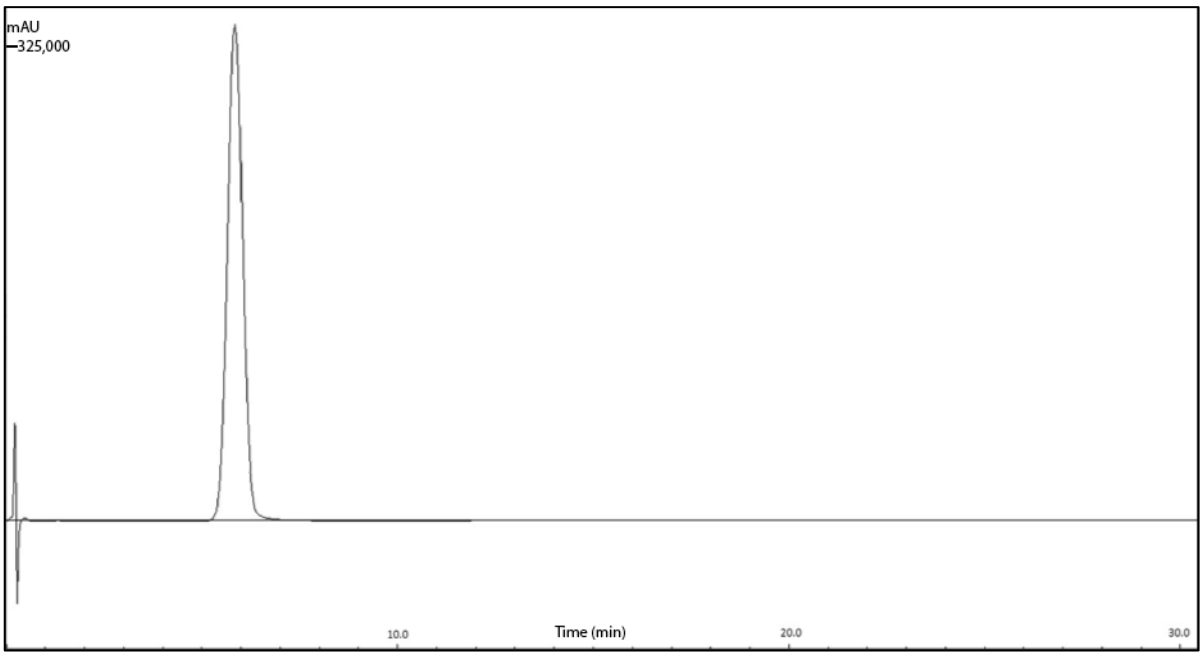

142 **Figure 2.** IAM chromatograms achieved for the analytes A) Paroxetine (50 µg $mL^{-1}$ in methanol)

143 and B) Diclofenac (50 µg $mL^{-1}$ in methanol). The mobile phase was a solution 70/30 v/v

144 Dulbecco's phosphate-buffered saline (DPBS) / methanol. The detailed experimental conditions are

145 reported in paragraph 4.0.

146 A

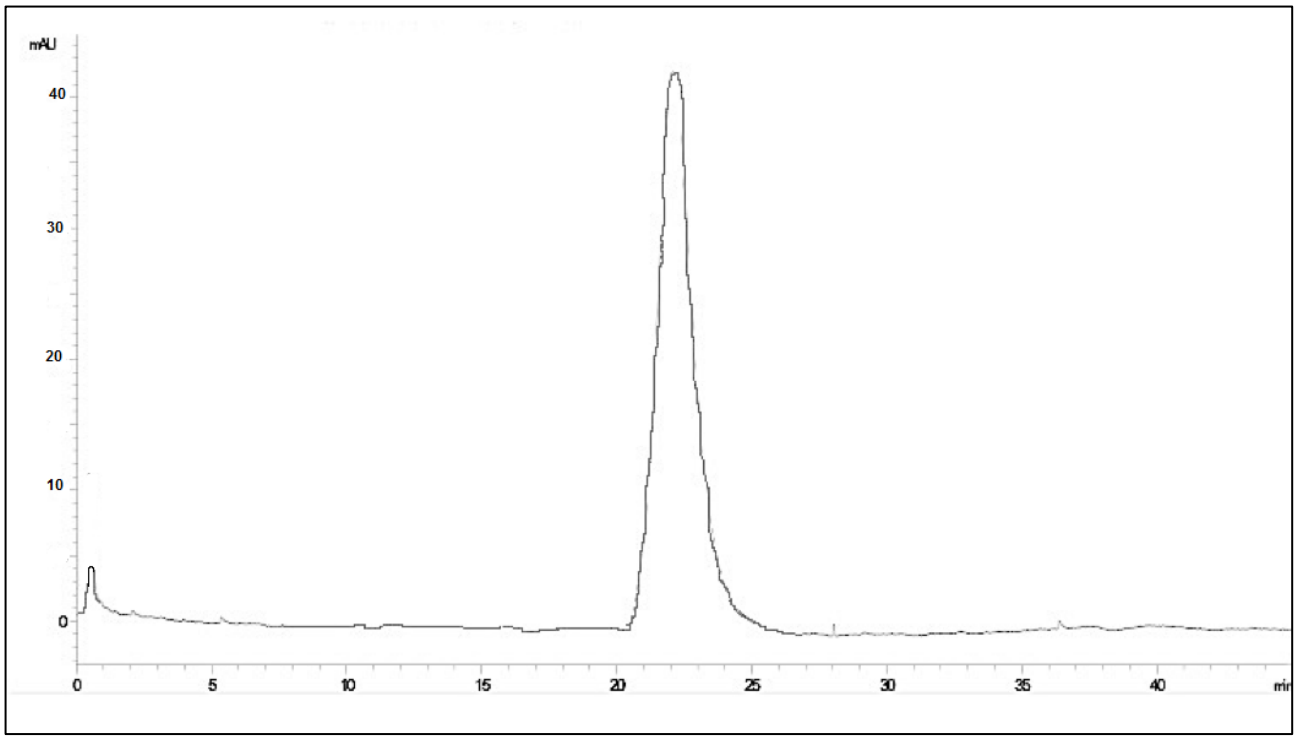


147
148

149 B

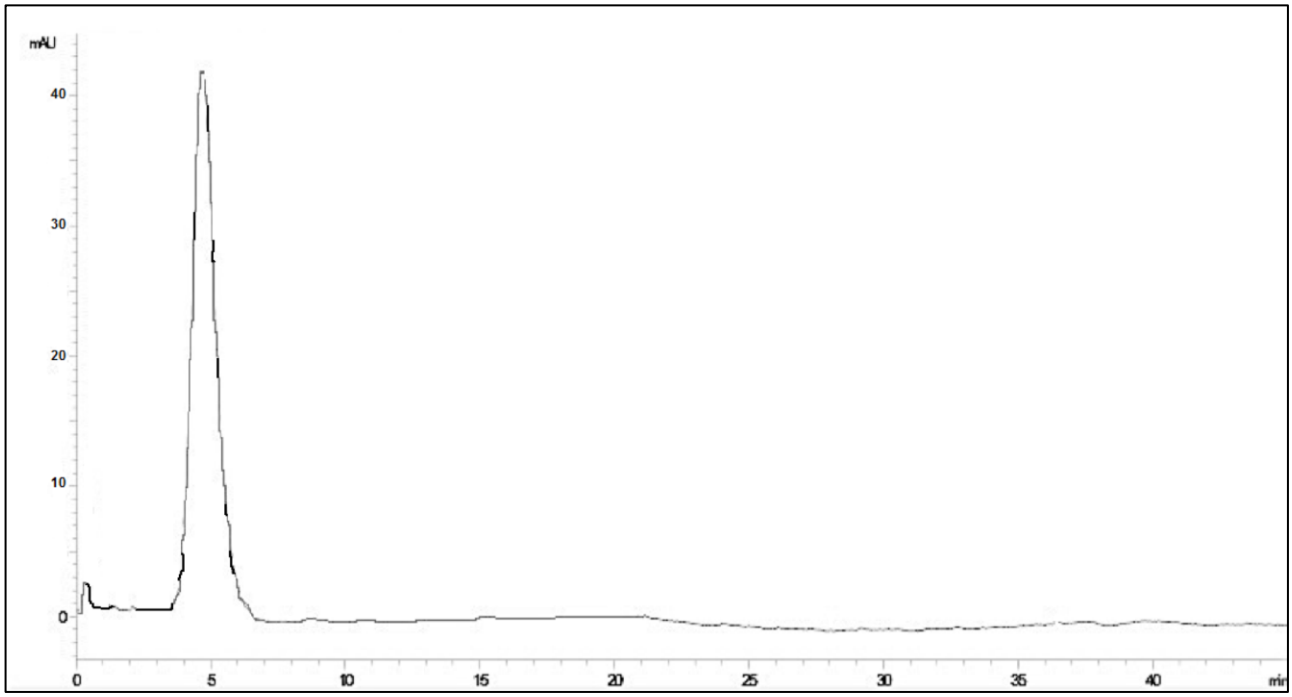


150

151 **Table 1.** pKa values, log $k_w^{SDS}$, log $k_{30\%MeOH}^{IAM}$ indexes, log BB values, experimental UV

152 wavelengths and suppliers for the analytes taken into account.

153

| Analyte | pKa | log $k_w^{SDS}$ | log $k_{30\%MeOH}^{IAM}$ | log BB | UV wavelength (nm) | Supplier |
|---|---|---|---|---|---|---|
| 2-(Methylamino)pyridine | - | 1.611 | -0.164 | -0.30[18] | 254 | Sigma-Aldrich |
| 2,2,2-trifluoroethyl vinyl ether | - | 0.929 | -0.142 | 0.13[18] | 210 | Sigma-Aldrich |
| 2,6-diisopropylphenol | - | 1.688 | 1.097 | 0.91[19] | 210 | TCI Europe |
| Acetaminophen | 9.69 | -0.092 | -0.204 | -1.00[19] | 254 | Acros Organics |
| Acetylsalicylic acid | 3.50 | -0.301 | -0.274 | -1.30[19] | 230 | Acros Organics |
| Aminopyrine | 5.03 | 1.486 | -0.206 | 0.00[19] | 254 | Sigma-Aldrich |
| Amitriptyline | 9.17 | 2.230 | 1.606 | 1.30[19] | 254 | TCI Europe |
| Amobarbital | 7.48/11.15* | 1.208 | 0.059 | 0.04[19] | 210 | Sigma-Aldrich |
| Antipyrine | 1.44 | 1.059 | -0.277 | -0.10[19] | 240 | Acros Organics |
| Atenolol | 9.19 | 1.156 | -0.162 | -1.00[19] | 270 | Acros Organics |
| Benzene | - | 1.202 | 0.036 | 0.37[20] | 210 | TCI Europe |
| Betahistine | 7.84 | 0.125 | -0.193 | -0.30[21] | 254 | Acros Organics |
| Caffeine | 0.60 | 0.910 | -0.284 | -0.06[19] | 210 | Acros Organics |
| Carbamazepine | - | 1.191 | 0.210 | 0.00[19] | 210 | Acros Organics |
| Celecoxib | 9.38 | 1.461 | 1.613 | -1.00[21] | 254 | Acros Organics |
| Chlorambucil | 4.60 | 0.787 | 0.308 | -1.70[19] | 254 | TCI Europe |
| Chlorpromazine | 9.50 | 2.169 | 2.038 | 1.36[21] | 254 | TCI Europe |
| Cimetidine | 7.01 | 1.003 | -0.177 | -1.42[19] | 210 | TCI Europe |
| Citalopram | 9.22 | 1.832 | 1.005 | 0.48[21] | 210 | TCI Europe |
| Clonidine | 8.08 | 1.436 | 0.171 | 0.11[19] | 270 | TCI Europe |
| Clozapine | 7.90 | 1.784 | 1.529 | 0.60[21] | 254 | TCI Europe |
| Cotinine | - | 1.424 | -0.260 | -0.32[19] | 260 | TCI Europe |
| Cyclobenzaprine | 8.47 | 2.092 | 1.607 | 1.08[21] | 230 | TCI Europe |
| Desipramine | 10.28 | 2.144 | 1.536 | 1.20[19] | 254 | Sigma-Aldrich |
| Diclofenac | 3.99 | 0.602 | 0.024 | -1.70[21] | 254 | Acros Organics |
| Diphenhydramine | 8.86 | 2.077 | 0.858 | 1.20[21] | 210 | Acros Organics |
| Domperidone | 9.68 | 1.937 | 1.562 | -0.78[19] | 270 | TCI Europe |

| | | | | | | |
|---|---|---|---|---|---|---|
| Donepezil | 8.54* | 1.968 | 0.858 | 0.89[22] | 210 | Acros Organics |
| Eserine | 8.17 | 1.656 | 0.030 | 0.08[19] | 240 | TCI Europe |
| Ethosuximide | 9.27 | 0.545 | -0.228 | 0.04[21] | 210 | Acros Organics |
| Ethylbenzene | - | 1.588 | 0.600 | 0.26[20] | 210 | Acros Organics |
| Fluphenazine | 7.84/2.08* | 2.207 | 2.066 | 1.51[19] | 254 | Sigma-Aldrich |
| Haloperidol | 8.29 | 2.366 | 1.483 | 1.34[22] | 254 | TCI Europe |
| Halothane | - | 1.215 | 0.152 | 0.35[20] | 210 | Sigma-Aldrich |
| Hexobarbital | 8.20 | 1.284 | -0.008 | 0.10[19] | 254 | Sigma-Aldrich |
| Hydroxyzine | 7.52/1.58* | 2.038 | 1.337 | 0.90[21] | 210 | Sigma-Aldrich |
| Ibuprofen | 4.24 | 0.626 | 0.090 | -0.18[19] | 270 | Acros Organics |
| Imipramine | 9.52 | 2.190 | 1.452 | 1.30[19] | 240 | Acros Organics |
| Indomethacin | 4.13 | 0.647 | -0.257 | -1.26[19] | 210 | TCI Europe |
| Ketorolac | 3.84 | -0.097 | -0.500 | -2.00[21] | 300 | TCI Europe |
| Lamotrigine | 5.36 | 1.316 | -0.006 | 0.48[23] | 220 | Acros Organics |
| Levofloxacin | 6.20/5.45* | 1.388 | -0.099 | -0.70[21] | 290 | TCI Europe |
| Metanol | - | 0.000 | -0.447 | 0.02[23] | 210 | Sigma-Aldrich |
| Metoclopramide | 9.71 | 1.610 | 0.346 | 0.08[21] | 210 | TCI Europe |
| Metoprolol | 9.56 | 1.771 | 0.198 | 1.15[22] | 220 | TCI Europe |
| Mianserin | 6.92 | 2.152 | 1.456 | 0.99[19] | 280 | TCI Europe |
| Naproxen | 4.14 | 0.153 | -0.090 | -1.70[21] | 254 | Acros Organics |
| Nicotine | 8.11 | 1.969 | -0.139 | 0.40[20] | 210 | Acros Organics |
| Nitrofurantoin | 7.05 | -0.074 | -0.447 | -2.00[21] | 254 | Acros Organics |
| Norfloxacin | 8.68/5.77* | 1.332 | -0.062 | -1.00[21] | 280 | Acros Organics |
| Nortriptyline | 10.13 | 2.169 | 1.639 | 1.04[21] | 254 | TCI Europe |
| Olanzapine | 7.80 | 1.825 | 0.843 | 0.80[21] | 254 | TCI Europe |
| Omeprazole | 9.29/4.77* | 1.591 | -0.229 | -0.82[19] | 300 | TCI Europe |
| Oxazepam | - | 1.420 | 0.707 | 0.61[19] | 230 | Sigma-Aldrich |
| Paroxetine | 9.77 | 2.104 | 1.796 | 0.48[21] | 210 | TCI Europe |
| Pentobarbital | 8.18 | 1.243 | 0.103 | 0.12[19] | 210 | Sigma-Aldrich |
| Phenylbutazone | 4.34 | 0.996 | 0.273 | -0.52[19] | 240 | Acros Organics |
| Phenytoin | 8.28 | 1.311 | 0.382 | -0.04[19] | 210 | Acros Organics |

| | | | | | | |
|---|---|---|---|---|---|---|
| Pindolol | 9.54 | 0.811 | 0.312 | 0.30[21] | 210 | Sigma-Aldrich |
| Primidone | - | 0.710 | -0.152 | -0.07[21] | 210 | TCI Europe |
| Promazine | 9.36 | 2.030 | 1.643 | 1.23[20] | 254 | Sigma-Aldrich |
| Promethazine | 9.00 | 2.040 | 1.613 | 1.30[24] | 254 | TCI Europe |
| Propranolol | 9.16 | 2.028 | 0.992 | 0.85[21] | 290 | Acros Organics |
| Quinidine | 8.56 | 2.245 | 0.982 | 0.33[22] | 230 | Acros Organics |
| Ranitidine | 8.33 | 1.233 | -0.239 | -1.23[19] | 230 | TCI Europe |
| Rifampicin | 1.70 | 1.900 | 0.990 | -1.52[21] | 230 | TCI Europe |
| Ropinirole | 10.17 | 1.685 | 0.326 | 0.25[19] | 254 | Sigma-Aldrich |
| Salicylic acid | 2.82 | -0.280 | -0.302 | -1.10[19] | 300 | Acros Organics |
| Theobromine | - | 0.347 | -0.284 | -0.28[19] | 270 | Acros Organics |
| Theophylline | - | 0.447 | -0.218 | -0.29[19] | 270 | Acros Organics |
| Toluene | - | 1.459 | 0.330 | 0.37[20] | 210 | Acros Organics |
| Tramadol | 9.41 | 1.692 | 0.256 | 0.70[21] | 210 | Sigma-Aldrich |
| Trazodone | 7.30 | 2.223 | 0.780 | 0.30[21] | 210 | Sigma-Aldrich |
| Triprolidine | 8.64 | 2.493 | 0.789 | 0.78[21] | 230 | Sigma-Aldrich |
| Valproic acid | 4.54 | 0.001 | -0.279 | -0.84[19] | 210 | Acros Organics |
| Venlafaxine | 9.67 | 1.900 | 0.429 | 0.48[25] | 230 | Acros Organics |
| Verapamil | 8.68 | 2.271 | 1.169 | -0.52[19] | 210 | Acros Organics |
| Zidovudine | 9.40 | 0.271 | -0.264 | -1.00[20] | 270 | Acros Organics |
| Zolmitriptan | 9.55 | 0.974 | -0.159 | -1.40[21] | 220 | TCI Europe |

* calculated by Marvin Sketch 15.1 software

158 **Table 2A.** Minimum and most populated values, expressed in kcal $mol^{-1}$, of the cluster affinities of

159 the analytes for the first four (from 1 to 4) discrete binding sites located on the P-gp.

160
161

| Analyte | P-gp 1 Min | P-gp 1 MP | P-gp 2 Min | P-gp 2 MP | P-gp 3 Min | P-gp 3 MP | P-gp 4 Min | P-gp 4 MP |
|---|---|---|---|---|---|---|---|---|
| 2-(Methylamino)pyridine | -3.03 | -3.03 | -3.61 | -3.61 | -3.62 | -3.62 | -3.63 | -3.63 |
| 2,2,2-trifluoroethyl vinyl ether | -1.72 | -1.72 | -2.09 | -2.09 | -1.85 | -1.85 | -1.98 | -1.94 |
| 2,6-diisopropylphenol | -4.42 | -4.42 | -5.36 | -5.36 | -5.55 | -5.55 | -5.36 | -5.36 |
| Acetaminophen | -3.30 | -3.30 | -4.72 | -4.72 | -4.13 | -4.08 | -4.85 | -4.85 |
| Acetylsalicylic acid | -3.57 | -3.57 | -4.47 | -4.36 | -4.48 | -4.48 | -4.22 | -3.95 |
| Aminopyrine | -4.43 | -4.30 | -5.66 | -5.66 | -5.63 | -5.63 | -5.70 | -5.70 |
| Amitriptyline | -6.09 | -5.02 | -7.29 | -7.15 | -6.39 | -6.39 | -7.22 | -7.22 |
| Amobarbital | -4.14 | -4.06 | -5.30 | -5.00 | -4.83 | -4.83 | -5.05 | -5.05 |
| Antipyrine | -4.33 | -4.33 | -5.61 | -5.61 | -5.31 | -5.31 | -5.61 | -5.44 |
| Atenolol | -3.81 | -3.34 | -5.74 | -3.99 | -3.82 | -3.40 | -4.83 | -4.70 |
| Benzene | -2.72 | -2.72 | -3.31 | -3.31 | -3.31 | -3.31 | -3.31 | -3.31 |
| Betahistine | -3.06 | -3.06 | -3.68 | -3.68 | -3.32 | -3.14 | -3.70 | -3.70 |
| Caffeine | -3.80 | -3.80 | -4.60 | -4.60 | -4.23 | -4.23 | -4.33 | -4.33 |
| Carbamazepine | -5.84 | -5.82 | -7.09 | -7.09 | -6.12 | -6.12 | -7.07 | -7.07 |
| Celecoxib | -4.30 | -4.30 | -7.01 | -6.98 | -4.73 | -4.12 | -7.18 | -7.18 |
| Chlorambucil | -3.77 | -3.77 | -5.13 | -4.81 | -5.19 | -5.19 | -5.16 | -5.16 |
| Chlorpromazine | -5.38 | -4.84 | -7.24 | -7.24 | -6.57 | -6.57 | -7.26 | -7.26 |
| Cimetidine | -3.27 | -2.95 | -4.74 | -4.60 | -4.10 | -4.02 | -4.70 | -4.64 |
| Citalopram | -4.75 | -4.45 | -6.41 | -6.14 | -4.93 | -4.93 | -7.16 | -6.86 |
| Clonidine | -4.34 | -4.34 | -5.41 | -5.41 | -5.44 | -5.44 | -5.40 | -5.40 |
| Clozapine | -5.10 | -5.05 | -7.01 | -7.01 | -5.36 | -5.36 | -7.00 | -6.98 |
| Cotinine | -3.93 | -3.87 | -5.14 | -4.79 | -4.92 | -4.92 | -4.82 | -4.82 |
| Cyclobenzaprine | -6.32 | -5.14 | -7.18 | -7.04 | -6.94 | -6.94 | -7.14 | -7.14 |
| Desipramine | -5.75 | -5.43 | -6.80 | -6.62 | -6.26 | -6.08 | -6.53 | -6.53 |
| Diclofenac | -5.23 | -4.96 | -6.34 | -6.13 | -6.49 | -6.19 | -6.14 | -6.05 |
| Diphenhydramine | -4.35 | -3.91 | -5.63 | -5.63 | -5.14 | -5.14 | -5.61 | -5.61 |
| Domperidone | -5.23 | -4.82 | -7.12 | -6.98 | -6.39 | -6.39 | -7.18 | -7.18 |
| Donepezil | -6.05 | -6.05 | -7.70 | -7.46 | -6.69 | -6.67 | -7.72 | -7.65 |
| Eserine | -4.88 | -4.88 | -6.01 | -5.87 | -5.45 | -5.45 | -5.91 | -5.91 |
| Ethosuximide | -3.62 | -3.62 | -4.22 | -4.22 | -4.47 | -4.39 | -4.42 | -4.42 |
| Ethylbenzene | -3.34 | -3.34 | -4.22 | -4.22 | -4.07 | -4.07 | -4.07 | -4.07 |
| Fluphenazine | -4.81 | -3.58 | -6.75 | -6.75 | -4.30 | -4.12 | -6.60 | -5.82 |
| Haloperidol | -4.35 | -4.17 | -6.25 | -6.25 | -5.60 | -5.60 | -7.23 | -6.20 |
| Halothane | -2.12 | -2.12 | -2.76 | -2.75 | -2.74 | -2.72 | -2.66 | -2.64 |
| Hexobarbital | -4.85 | -4.79 | -6.02 | -6.02 | -5.13 | -4.97 | -6.03 | -6.03 |
| Hydroxyzine | -4.24 | -3.67 | -6.41 | -5.43 | -4.05 | -3.66 | -6.19 | -5.84 |
| Ibuprofen | -4.37 | -4.37 | -5.52 | -5.43 | -5.88 | -5.88 | -5.43 | -5.34 |
| Imipramine | -5.34 | -5.34 | -6.68 | -6.68 | -5.76 | -4.64 | -6.68 | -6.13 |
| Indomethacin | -5.67 | -5.53 | -7.02 | -7.02 | -7.28 | -7.28 | -7.37 | -7.37 |
| Ketorolac | -5.22 | -5.22 | -6.61 | -6.61 | -6.55 | -6.41 | -6.62 | -6.62 |
| Lamotrigine | -4.49 | -3.92 | -5.84 | -5.84 | -4.88 | -4.56 | -5.36 | -5.36 |
| Levofloxacin | -4.45 | -4.45 | -5.80 | -5.54 | -5.80 | -5.23 | -6.07 | -5.85 |
| Metanol | -1.40 | -1.33 | -1.43 | -1.43 | -1.33 | -1.33 | -1.40 | -1.40 |

| | | | | | | | | |
|---|---|---|---|---|---|---|---|---|
| Metoclopramide | -3.47 | -3.47 | -5.19 | -3.92 | -3.71 | -3.07 | -4.52 | -4.13 |
| Metoprolol | -3.58 | -3.35 | -4.63 | -4.06 | -3.54 | -2.87 | -4.39 | -4.18 |
| Mianserin | -5.23 | -5.23 | -7.06 | -7.06 | -6.05 | -5.98 | -7.11 | -7.11 |
| Naproxen | -4.82 | -4.82 | -5.99 | -5.99 | -6.03 | -5.91 | -6.03 | -6.03 |
| Nicotine | -4.02 | -4.02 | -4.70 | -4.69 | -4.50 | -4.50 | -4.70 | -4.70 |
| Nitrofurantoin | -4.10 | -4.10 | -5.33 | -5.33 | -5.18 | -5.18 | -5.32 | -5.32 |
| Norfloxacin | -3.83 | -3.83 | -5.59 | -5.59 | -5.51 | -5.51 | -5.75 | -5.63 |
| Nortriptyline | -6.35 | -6.35 | -7.07 | -6.86 | -6.44 | -6.44 | -7.00 | -7.00 |
| Olanzapine | -4.60 | -4.60 | -6.71 | -6.62 | -5.47 | -5.29 | -6.68 | -6.68 |
| Omeprazole | -5.26 | -5.20 | -6.96 | -6.76 | -6.65 | -6.41 | -7.16 | -6.92 |
| Oxazepam | -5.29 | -5.29 | -6.90 | -6.90 | -6.16 | -6.16 | -6.89 | -6.89 |
| Paroxetine | -4.94 | -4.94 | -6.95 | -6.84 | -6.42 | -5.67 | -6.83 | -6.29 |
| Pentobarbital | -3.88 | -3.88 | -4.76 | -4.76 | -4.41 | -4.41 | -4.91 | -4.91 |
| Phenylbutazone | -5.53 | -5.53 | -7.27 | -7.27 | -6.02 | -5.12 | -7.45 | -6.69 |
| Phenytoin | -5.00 | -5.00 | -6.56 | -6.56 | -5.39 | -5.00 | -6.55 | -6.55 |
| Pindolol | -4.17 | -4.13 | -5.43 | -4.86 | -4.56 | -4.26 | -5.47 | -4.60 |
| Primidone | -4.55 | -4.55 | -5.19 | -5.19 | -4.88 | -4.71 | -5.50 | -5.50 |
| Promazine | -5.58 | -5.58 | -6.79 | -6.50 | -6.32 | -6.32 | -6.50 | -5.84 |
| Promethazine | -4.99 | -4.80 | -6.78 | -6.49 | -6.60 | -5.83 | -6.51 | -6.42 |
| Propranolol | -4.60 | -4.38 | -6.33 | -5.54 | -4.79 | -4.22 | -6.10 | -5.39 |
| Quinidine | -5.72 | -5.72 | -7.43 | -7.43 | -5.26 | -4.56 | -7.77 | -7.77 |
| Ranitidine | -2.77 | -2.65 | -4.11 | -3.91 | -4.42 | -2.88 | -4.31 | -3.48 |
| Rifampicin | -7.10 | -6.50 | -4.48 | -4.32 | -6.80 | -5.95 | -7.22 | -6.59 |
| Ropinirole | -4.02 | -4.01 | -6.30 | -5.55 | -4.72 | -3.94 | -5.94 | -5.52 |
| Salicylic acid | -3.09 | -3.09 | -3.69 | -3.69 | -4.00 | -4.00 | -3.74 | -3.71 |
| Theobromine | -3.47 | -3.47 | -4.54 | -4.54 | -4.08 | -4.08 | -4.54 | -4.54 |
| Theophylline | -3.63 | -3.63 | -4.43 | -4.43 | -3.88 | -3.87 | -4.43 | -4.43 |
| Toluene | -3.08 | -3.08 | -3.81 | -3.81 | -3.77 | -3.77 | -3.74 | -3.74 |
| Tramadol | -4.89 | -4.89 | -5.94 | -5.20 | -5.15 | -3.77 | -5.71 | -5.30 |
| Trazodone | -5.37 | -5.00 | -7.30 | -5.74 | -5.79 | -6.47 | -7.09 | -6.06 |
| Triprolidine | -5.03 | -4.92 | -7.19 | -7.11 | -5.36 | -5.36 | -6.96 | -6.88 |
| Valproic acid | -2.78 | -2.78 | -3.56 | -3.56 | -3.81 | -3.81 | -3.43 | -3.43 |
| Venlafaxine | -4.81 | -4.54 | -6.07 | -5.82 | -4.54 | -4.09 | -6.47 | -6.08 |
| Verapamil | -3.93 | -3.54 | -6.56 | -6.37 | -5.28 | -4.48 | -6.58 | -6.14 |
| Zidovudine | -3.45 | -3.21 | -5.14 | -5.14 | -3.56 | -3.27 | -5.20 | -5.20 |
| Zolmitriptan | -4.48 | -4.32 | -6.32 | -6.01 | -5.56 | -5.56 | -6.38 | -5.73 |

163 **Table 2B.** Minimum and most populated values, expressed as kcal $mol^{-1}$, of the cluster affinities of

164 the analytes for the second four (from 5 to 8) discrete binding sites located on the P-gp.

165

| Analyte | P-gp 5 Min | P-gp 5 MP | P-gp 6 Min | P-gp 6 MP | P-gp 7 Min | P-gp 7 MP | P-gp 8 Min | P-gp 8 MP |
|---|---|---|---|---|---|---|---|---|
| 2-(Methylamino)pyridine | -3.03 | -3.03 | -3.40 | -3.40 | -3.53 | -3.53 | -3.22 | -3.22 |
| 2,2,2-trifluoroethyl vinyl ether | -1.72 | -1.64 | -2.05 | -2.05 | -2.18 | -2.18 | -1.93 | -1.93 |
| 2,6-diisopropylphenol | -4.42 | -4.22 | -5.17 | -5.17 | -5.56 | -5.56 | -4.67 | -4.67 |
| Acetaminophen | -3.81 | -3.81 | -4.20 | -4.20 | -4.10 | -4.10 | -3.37 | -3.37 |
| Acetylsalicylic acid | -3.86 | -3.86 | -3.91 | -3.91 | -4.42 | -4.42 | -3.68 | -3.68 |
| Aminopyrine | -5.20 | -5.18 | -5.36 | -4.91 | -5.60 | -5.60 | -4.47 | -4.47 |
| Amitriptyline | -6.00 | -5.92 | -6.85 | -6.85 | -7.49 | -7.49 | -5.63 | -5.63 |
| Amobarbital | -4.51 | -4.51 | -4.40 | -4.05 | -4.99 | -4.99 | -4.23 | -4.23 |
| Antipyrine | -4.78 | -4.78 | -4.77 | -4.77 | -5.58 | -5.58 | -4.31 | -4.30 |
| Atenolol | -4.03 | -4.03 | -4.82 | -4.60 | -4.86 | -4.86 | -3.37 | -3.37 |
| Benzene | -3.19 | -3.19 | -3.26 | -3.26 | -3.31 | -3.31 | -3.01 | -3.01 |
| Betahistine | -2.93 | -2.93 | -3.54 | -3.54 | -3.52 | -3.52 | -3.41 | -3.41 |
| Caffeine | -3.64 | -3.64 | -3.76 | -3.76 | -4.56 | -4.56 | -3.76 | -3.76 |
| Carbamazepine | -5.87 | -5.87 | -6.16 | -6.16 | -6.83 | -6.83 | -5.31 | -5.31 |
| Celecoxib | -5.93 | -5.31 | -5.82 | -5.82 | -7.97 | -7.97 | -5.59 | -5.04 |
| Chlorambucil | -4.30 | -4.30 | -4.57 | -4.56 | -5.63 | -5.63 | -3.93 | -3.93 |
| Chlorpromazine | -5.66 | -5.00 | -6.75 | -6.57 | -7.23 | -7.01 | -5.16 | -5.16 |
| Cimetidine | -3.72 | -3.45 | -4.58 | -3.80 | -4.76 | -3.88 | -3.41 | -3.20 |
| Citalopram | -5.63 | -5.59 | -5.85 | -5.69 | -6.44 | -6.44 | -4.93 | -4.86 |
| Clonidine | -4.06 | -3.98 | -4.47 | -4.40 | -5.34 | -5.34 | -4.31 | -4.31 |
| Clozapine | -5.44 | -5.18 | -6.64 | -6.64 | -7.05 | -7.05 | -4.98 | -4.95 |
| Cotinine | -4.52 | -4.52 | -4.48 | -4.48 | -4.86 | -4.76 | -4.29 | -4.29 |
| Cyclobenzaprine | -5.70 | -5.68 | -7.12 | -6.86 | -7.35 | -7.23 | -5.36 | -5.28 |
| Desipramine | -5.74 | -5.74 | -6.44 | -6.44 | -6.42 | -5.73 | -4.78 | -4.78 |
| Diclofenac | -5.23 | -5.23 | -5.96 | -5.46 | -6.32 | -6.32 | -4.65 | -4.37 |
| Diphenhydramine | -5.07 | -5.07 | -5.41 | -4.78 | -5.42 | -5.42 | -3.89 | -3.54 |
| Domperidone | -6.04 | -5.71 | -5.73 | -5.73 | -7.69 | -7.69 | -6.26 | -6.13 |
| Donepezil | -7.11 | -6.10 | -7.07 | -7.07 | -7.83 | -7.77 | -6.58 | -6.58 |
| Eserine | -5.52 | -5.50 | -5.57 | -5.57 | -5.92 | -5.92 | -4.57 | -4.54 |
| Ethosuximide | -3.62 | -3.62 | -4.16 | -4.16 | -4.34 | -4.34 | -3.76 | -3.35 |
| Ethylbenzene | -3.58 | -3.58 | -3.96 | -3.96 | -4.21 | -4.21 | -3.71 | -3.71 |
| Fluphenazine | -4.39 | -4.39 | -5.23 | -3.06 | -6.46 | -5.16 | -5.79 | -5.79 |
| Haloperidol | -5.68 | -5.14 | -5.35 | -4.41 | -7.32 | -7.31 | -5.48 | -5.35 |
| Halothane | -2.37 | -2.37 | -2.57 | -2.55 | -2.86 | -2.86 | -2.41 | -2.35 |
| Hexobarbital | -5.21 | -4.99 | -5.22 | -5.22 | -5.51 | -5.51 | -4.56 | -4.50 |
| Hydroxyzine | -5.26 | -4.29 | -5.29 | -5.29 | -6.18 | -5.89 | -4.57 | -4.50 |
| Ibuprofen | -4.84 | -4.84 | -4.91 | -4.69 | -5.41 | -5.41 | -4.55 | -4.55 |
| Imipramine | -5.83 | -5.18 | -6.69 | -6.32 | -6.67 | -6.67 | -4.97 | -4.97 |

| | | | | | | | | |
|---|---|---|---|---|---|---|---|---|
| Indomethacin | -5.92 | -5.92 | -6.44 | -6.44 | -7.22 | -6.91 | -5.26 | -5.26 |
| Ketorolac | -5.73 | -5.68 | -5.71 | -5.63 | -6.36 | -6.35 | -5.01 | -4.74 |
| Lamotrigine | -4.13 | -4.09 | -4.77 | -4.77 | -5.30 | -5.23 | -4.32 | -3.66 |
| Levofloxacin | -5.40 | -5.14 | -3.46 | -3.46 | -6.37 | -6.37 | -4.71 | -4.71 |
| Metanol | -1.47 | -1.47 | -1.38 | -1.38 | -1.37 | -1.37 | -1.42 | -1.42 |
| Metoclopramide | -3.63 | -3.36 | -4.40 | -4.02 | -4.95 | -4.95 | -3.55 | -2.80 |
| Metoprolol | -3.49 | -3.46 | -4.25 | -4.25 | -4.60 | -4.39 | -3.57 | -3.42 |
| Mianserin | -5.89 | -5.89 | -6.21 | -6.21 | -7.07 | -7.07 | -5.63 | -5.63 |
| Naproxen | -5.26 | -5.26 | -5.48 | -5.48 | -5.80 | -5.80 | -4.72 | -4.71 |
| Nicotine | -3.77 | -3.77 | -4.42 | -4.20 | -4.67 | -4.67 | -4.24 | -4.13 |
| Nitrofurantoin | -4.37 | -4.30 | -4.62 | -4.31 | -5.24 | -5.24 | -3.90 | -3.67 |
| Norfloxacin | -4.46 | -4.44 | -3.73 | -2.70 | -5.85 | -5.83 | -4.99 | -4.99 |
| Nortriptyline | -5.98 | -5.98 | -7.20 | -7.20 | -7.09 | -7.07 | -5.30 | -5.05 |
| Olanzapine | -5.42 | -5.42 | -6.24 | -6.24 | -6.48 | -6.48 | -5.06 | -5.06 |
| Omeprazole | -5.24 | -5.22 | -6.47 | -6.47 | -7.26 | -6.79 | -5.28 | -4.22 |
| Oxazepam | -5.96 | -5.94 | -6.61 | -6.61 | -6.81 | -6.70 | -5.02 | -5.02 |
| Paroxetine | -5.71 | -5.03 | -6.14 | -4.23 | -7.49 | -6.50 | -4.97 | -4.97 |
| Pentobarbital | -4.29 | -4.18 | -4.35 | -4.22 | -4.84 | -4.84 | -3.75 | -3.60 |
| Phenylbutazone | -6.29 | -6.19 | -7.19 | -7.19 | -7.33 | -6.78 | -5.57 | -5.44 |
| Phenytoin | -5.80 | -5.80 | -5.42 | -5.38 | -6.25 | -6.25 | -4.67 | -4.64 |
| Pindolol | -3.61 | -3.58 | -5.72 | -5.72 | -5.29 | -5.13 | -4.03 | -3.81 |
| Primidone | -4.43 | -4.31 | -4.99 | -4.99 | -5.23 | -5.23 | -4.26 | -4.08 |
| Promazine | -5.47 | -4.86 | -6.22 | -5.94 | -6.47 | -6.05 | -4.71 | -4.50 |
| Promethazine | -5.55 | -4.99 | -6.07 | -5.87 | -6.62 | -6.40 | -4.72 | -4.68 |
| Propranolol | -4.42 | -4.42 | -5.99 | -5.19 | -5.67 | -5.62 | -4.30 | -4.30 |
| Quinidine | -5.68 | -5.68 | -6.74 | -5.62 | -7.92 | -7.78 | -5.32 | -4.72 |
| Ranitidine | -2.99 | -2.99 | -3.61 | -3.34 | -3.76 | -2.86 | -2.12 | -1.63 |
| Rifampicin | -5.13 | -3.28 | -6.66 | -6.00 | -7.44 | -7.00 | -3.14 | -3.14 |
| Ropinirole | -4.25 | -4.17 | -5.98 | -5.98 | -6.22 | -6.22 | -4.11 | -3.39 |
| Salicylic acid | -3.09 | -3.09 | -3.42 | -3.42 | -3.85 | -3.85 | -3.31 | -3.31 |
| Theobromine | -3.46 | -3.46 | -3.49 | -3.49 | -4.29 | -4.29 | -3.80 | -3.80 |
| Theophylline | -3.63 | -3.63 | -3.72 | -3.72 | -4.45 | -4.45 | -3.66 | -3.66 |
| Toluene | -3.42 | -3.42 | -3.79 | -3.79 | -3.93 | -3.93 | -3.39 | -3.39 |
| Tramadol | -4.46 | -4.46 | -5.36 | -5.36 | -5.62 | -5.46 | -4.26 | -4.26 |
| Trazodone | -6.06 | -6.26 | -6.86 | -6.86 | -7.40 | -7.29 | -6.06 | -5.47 |
| Triprolidine | -6.48 | -6.48 | -6.40 | -5.53 | -7.28 | -7.28 | -5.38 | -5.26 |
| Valproic acid | -3.03 | -3.03 | -3.10 | -3.10 | -3.76 | -3.76 | -2.90 | -2.90 |
| Venlafaxine | -4.64 | -4.33 | -5.60 | -5.23 | -6.48 | -6.48 | -4.40 | -4.40 |
| Verapamil | -5.16 | -4.84 | -4.74 | -3.51 | -6.80 | -6.53 | -4.32 | -3.72 |
| Zidovudine | -3.94 | -3.93 | -4.49 | -4.49 | -4.55 | -4.55 | -3.90 | -3.19 |
| Zolmitriptan | -4.78 | -3.70 | -6.13 | -6.13 | -6.15 | -6.15 | -4.42 | -4.42 |

167 2.1 MLC INDEXES IN LOG BB PREDICTION

168 MLC indexes were used to develop BBB passage potential predicting models along with either
169 static or conformational properties. At first, all the analytes were assumed as having zero atomic
170 charges, even the ones supporting one or more ionizable functions. The equations along with the
171 statistical validation are reported in Table 3. In the equations thereby reported, $r^2$ is the multiple
172 regression coefficient, $q^2$ is the $r^2$ validated by Leave-One-Out (LOO) optimization, *SE* is the error
173 standard deviation, *F* represents the Fischer regression statistical value, *PC* is the Amemiya
174 predictive criterion and ExRow is the analyte excluded for maximizing the predictive strength of
175 the statistical model. If not differently indicated, every regression was developed by employing four
176 different independent variables (MLC indexes + three other physico-chemical descriptors).
177 Surprisingly, even if over two thirds of the analytes support one or more ionizable functions, fairly
178 good relationships, as the one expressed by equations (1) and (2), are obtained even not taking into
179 account the presence of electric charges. This may be attributed to the fact that, although the
180 molecular mechanisms involved in MLC are multiple and complex, the occurrence of
181 analyte/micelles electrostatic interactions plays a pivotal role in the global retention and it appears
182 reasonable to assume that such interactions are encoded in MLC indexes. It should be also
183 highlighted that, in these specific cases, being VirtualLogP values calculated starting from the
184 analytes assumed in their forms having zero atomic charges, such values can be reasonably assumed
185 as estimates of their log $P^N$ values. Subsequently, the analytes supporting extensively ionizable
186 functions (i.e. carboxy groups, for acids primary, secondary and tertiary amines for bases) were
187 assumed as completely charged, regardless of the relative abundance of the charged species at the
188 physiological pH. Considering the ionizable analytes as entirely charged species slightly worsened
189 the relationships (equations (3) and (4)). It should be pointed out that verapamil, the analyte
190 excluded to maximize the predictive strength of the statistical model is a well-known P-gp
191 substrate[26]. P-gp is an ATP-dependent efflux pump, with broad substrate specificity which pumps
192 many foreign substances out of cells[27]. Although it is widely expressed in the intestinal epithelium,

193 liver cells and proximal tubule of the kidney, P-gp is also localized in the capillary endothelial cells
194 composing the BBB and is responsible, for some classes of actives, of multi-drug resistance.
195 Eventually, a weighted average of the static properties at physiological pH (7.4), according to the
196 pKa of each compound, was performed. For zwitterions, the static properties were calculated for
197 each microspecies possibly present at pH 7.4 and their relative abundances, calculated by the
198 software Marvin Sketch 15.1 for Mac OS X[28], were also used to perform the weighted averages.
199 The relative abundances of the microspecies present at pH 7.4 are reported in the Supporting
200 Information section for the ampholytes levofloxacin (page S-2), norfloxacin (page S-4) and
201 omeprazole (page S-6). This approach was adapted to mirror more closely what actually occurs *in*
202 *vivo*. Performing the weighted average of the properties benefited noticeably the relationships as
203 described by equations (5) and (6). It is also interesting to note how, according to the above
204 reported relationships, the BBB penetration of drugs will be enhanced for highly retained
205 compounds in MLC, how it is hindered by the occurrence of drug/membrane polar (Psa)/
206 electrostatic (Dipole) interactions, and how the transport through the barrier seems favored for
207 bases (Charge). However, by taking into account the analytes assumed as static, the properties are
208 derived considering them in their minimum energy conformations, i.e. after minimization. Indeed,
209 several authors[29] reported that such conformations are not always the ones actually involved in
210 membrane barrier passage. Therefore, a conformational analysis *in vacuum* was carried out for each
211 analyte included in the data set by using the *Boltzmann Jump* method that generates at random 1000
212 possible conformations by exploring the conformational space of the rotatable dihedral angles. The
213 conformational analysis was first performed on the analytes assumed as having zero atomic
214 charges, then on the analytes assumed as completely charged and finally taking into account a
215 weighted average of the properties at the experimental pH 7.4, according to the pKa of each analyte.
216 In the following models the conformational properties were considered separately to look into the
217 predictive strength of the models. As it is evident from Table 3, the use of conformational
218 properties instead of the static ones slightly worsened the relationships. This aspect is quite

interesting as the calculation of conformational properties can be rather time-consuming especially if the compound libraries to screen are wide and the computers employed are not sufficiently powerful. Conversely, the static properties are much faster to calculate. Performing the weighted average of the conformational properties yielded the most predictive models (equations (11) and (12)) and in those relationships, verapamil again behaved as an *outlier*, suggesting that such models would not be able to mirror the penetration of analytes undergoing some sort of active transport, in this case P-gp mediated efflux. It is interesting to point out how, among the ionized properties employed for the statistical method development (equations (9) and (10)), no one depends noticeably on ionization. Furthermore, the conformational analysis demonstrated how it is the PSA Max, i.e. the maximum value that the PSA assumes by exploring the conformational space *in vacuum* of each analyte, that best relates with log BB values as those values are incorporated in each model based on conformational properties (equations (7), (8), (9), (10), (11) and (12)).

232 **Table 3.** Statistical validation of the models developed employing log $k_w^{SDS}$ values of the dataset

233 (*n*=79) along with three other physico-chemical descriptors.

234

| MOLECULAR DESCRIPTORS | $r^2$ | $q^2$ | *SE* | *F* | *PC* | $r^2$ (n-1) | *SE* (n-1) | *F* (n-1) | *PC* (n-1) | EX-ROW | EQUATIONS | EQ No |
|---|---|---|---|---|---|---|---|---|---|---|---|---|
| STATIC | | | | | | | | | | | | |
| ZERO ATOMIC CHARGES PROPERTIES | 0.69 | 0.65 | 0.521 | 41.42 | 21.656 | 0.71 | 0.510 | 44.06 | 20.535 | - | log BB = -0.2693 + 0.8191 log $k_w^{SDS}$ - 0.0162 Psa - 0.0824 VirtualLogP + 0.1456 HbDon | 1 |
| | | | | | | | | | | 2-(Methylamino) pyridine | log BB = -0.2166 + 0.8383 log $k_w^{SDS}$ - 0.0170 Psa - 0.0994 VirtualLogP + 0.1570 HbDon | 2 |
| IONIZED PROPERTIES | 0.68 | 0.63 | 0.530 | 39.28 | 22.452 | 0.70 | 0.517 | 42.20 | 21.104 | - | log BB = -0.3460 + 0.6671 log $k_w^{SDS}$ - 0.0104 Psa + 0.1425 Charge - 0.0138 Impropers | 3 |
| | | | | | | | | | | Verapamil | log BB = -0.4024 + 0.7071 log $k_w^{SDS}$ - 0.0093 Psa + 0.1297 Charge - 0.0187 Impropers | 4 |
| WEIGHTED AVERAGE | 0.72 | 0.68 | 0.498 | 47.05 | 19.795 | 0.73 | 0.486 | 50.29 | 18.617 | - | log BB = -0.3145 + 0.6825 log $k_w^{SDS}$ - 0.0091 Psa - 0.0202 Dipole + 0.2042 Charge | 5 |
| | | | | | | | | | | Verapamil | log BB = -0.3145 + 0.6825 log $k_w^{SDS}$ - 0.0091 Psa - | 6 |

| | | | | | | | | | | | | |
|---|---|---|---|---|---|---|---|---|---|---|---|---|
| | | | | | | | | | | | 0.0202 Dipole + 0.2042 Charge | |
| CONFORMATIONAL | | | | | | | | | | | | |
| ZERO ATOMIC CHARGES PROPERTIES | 0.69 | 0.64 | 0.526 | 40.25 | 22.081 | 0.71 | 0.509 | 44.37 | 20.426 | - | log BB = - 0.4857 + 0.8201 log $k_w^{SDS}$ - 0.0044 PSA Max - 0.0708 MD Max - 0.2671 MD sd | 7 |
| | | | | | | | | | | Pindolol | log BB = - 0.4973 + 0.8307 log $k_w^{SDS}$ - 0.0048 PSA Max - 0.0583 MD Max - 0.3274 MD sd | 8 |
| IONIZED PROPERTIES | 0.65 | 0.62 | 0.549 | 69.77 | 23.504 | 0.67 | 0.538 | 74.60 | 22.304 | - | log BB = - 0.5392 + 0.7898 log $k_w^{SDS}$ - 0.0093 PSA Max | 9 |
| | | | | | | | | | | Primidone | log BB = - 0.5338 + 0.8008 log $k_w^{SDS}$ - 0.0099 PSA Max | 10 |
| WEIGHTED AVERAGE | 0.68 | 0.63 | 0.534 | 38.57 | 22.729 | 0.70 | 0.520 | 41.69 | 21.283 | - | log BB = - 0.4329 + 0.7969 log $k_w^{SDS}$ - 0.0072 PSA Max - 0.0235 MD Min - 0.0485 MLP Average | 11 |
| | | | | | | | | | | Verapamil | log BB = - 0.4911 + 0.8121 log $k_w^{SDS}$ - 0.0068 PSA Max - 0.0233 MD Min - 0.0334 MLP Average | 12 |

## 2.2 IAM INDEXES IN LOG BB PREDICTION

The same approach was extended to the IAM indexes. The equations along with the statistical validation coefficient are reported in Table 4. Indeed, taking into account either the properties of the analytes assumed as having zero atomic charges (equations (13) and (14)) or those of the analytes

239 assumed as completely charged (equations (15) and (16)) resulted in a BBB passage predictive
240 strength inferior to that obtained by using MLC indexes. Such conclusions are supported by the
241 lower correlation coefficients obtained. It is interesting to note how domperidone, the compound
242 excluded in first best optimized model described by equation (14), is a well-known substrate of the
243 P-gp[26], and is pumped out of cells by such efflux system despite its high biomembrane passive
244 diffusion. Analogously to what was observed in the analysis of MLC indexes, performing the
245 weighted average of the static properties resulted the winning strategy also for this set of
246 experimental measures. In fact, a 0.72 $r^2$ ($n$-1), achieved on a set as large as 79 analytes, employing
247 only four descriptors suggests that the model (equations (17) and (18)) is robust and reliable
248 However, these relationships are roughly comparable to those obtained by using MLC indexes
249 (equations (5) and (6)). This evidence is indeed rather surprising, since the IAM stationary phase
250 consists of analogues of phosphatidylcholine, the most abundant phospholipid expressed in the
251 capillary endothelium acting as a barrier between the blood and the cerebrospinal fluids (CSF), and
252 thus they would represent an ideal biomimetic system. Conversely, this kind of SDS based MLC
253 should have drawbacks arising from the different chemical structure of SDS in comparison with
254 membrane phospholipids. But this evidence would suggest that they are incidentally able to mirror
255 the drug/membrane interactions involved *in vivo* thanks to the peculiar amphiphilic features of the
256 anionic micelles. In fact, for some reasons, they seem to be able to model the passive BBB
257 penetration of drugs fairly better than IAM indexes. Furthermore, the physico-chemical descriptors
258 reported in equation (18) are the same as the ones in equation (6), supporting again the concept
259 according to which the polar (Psa) /electrostatic (Dipole) interaction component plays a relevant
260 role in hindering the BBB penetration of drugs. Again, bases seem to be favored in BBB entering
261 and this is also consistent with the clinical experience. In fact, polar and extensively protonated at
262 pH 7.4 basic compounds, such as amphetamine and methamphetamine, are known to have an
263 appreciable CNS activity but it is much harder to recall similar cases for polar acids. The
264 conformational analyses of the analytes neither assumed as having zero atomic charges, nor as

265 ionized benefitted the relationships. Moreover, even performing the weighted average was not
266 beneficial at all for the relationships (data not shown).

267

**Table 4.** Statistical validation of the models developed employing log $k_{30\%\ MeOH}^{IAM}$ values of the dataset (*n*=79) along with three other physico-chemical descriptors.

| MOLECULAR DESCRIPTORS | $r^2$ | $q^2$ | *SE* | *F* | *PC* | $r^2$ (n-1) | *SE* (n-1) | *F* (n-1) | *PC* (n-1) | EX-ROW | EQUATIONS | EQ No |
|---|---|---|---|---|---|---|---|---|---|---|---|---|
| STATIC | | | | | | | | | | | | |
| ZERO ATOMIC CHARGES PROPERTIES | 0.64 | 0.59 | 0.561 | 33.08 | 25.156 | 0.67 | 0.540 | 36.88 | 23.025 | - | log BB = +0.6691 + 0.8369 log $k_{30\%\ MeOH}^{IAM}$ - 0.0166 Psa - 0.1473 VirtualLogP + 0.1139 HbDon | 13 |
| | | | | | | | | | | Domperidone | log BB = +0.6706 + 0.9057 log $k_{30\%\ MeOH}^{IAM}$ - 0.0161 Psa - 0.1473 VirtualLogP + 0.1173 HbDon | 14 |
| IONIZED PROPERTIES | 0.64 | 0.58 | 0.561 | 33.07 | 25.155 | 0.67 | 0.540 | 37.29 | 22.976 | - | log BB = -0.3460 + 0.5276 log $k_{30\%\ MeOH}^{IAM}$ + 0.0680 HbAcc - 0.0164 Psa - 0.3020 Charge | 15 |
| | | | | | | | | | | Lamotrigine | log BB = 0.3429 + 0.5324 log $k_{30\%\ MeOH}^{IAM}$ + 0.1027 HbAcc + 0.3288 Charge - 0.0188 Psa | 16 |
| WEIGHTED AVERAGE | 0.70 | 0.65 | 0.515 | 42.79 | 21.169 | 0.72 | 0.494 | 47.40 | 19.219 | - | log BB = +0.4388 + 0.5458 log $k_{30\%\ MeOH}^{IAM}$ - 0.0110 Psa - 0.0190 Dipole + 0.4653 Charge | 17 |
| | | | | | | | | | | Celecoxib | log BB = +0.3773 + 0.6063 log $k_{30\%\ MeOH}^{IAM}$- 0.0097 Psa - 0.0207 Dipole + 0.4182 Charge | 18 |

## 2.3 IAM + MLC INDEXES IN LOG BB PREDICTION

In the present study, MLC and IAM indexes were, in a first instance, considered separately. However, the evident differences in the elution order observed depict a rather different selectivity between both techniques. For this reason, the development of the BBB entering potential statistical models was also performed by considering both the chromatographic indexes at the same time, along with three other molecular descriptors (five independent variables in total), starting from the weighted average of the molecular properties. This strategy resulted in a markedly improved predictive strength (equations (19) and (20)) as reported in Table 5. These relationships may suggest that the molecular mechanism involved in IAM-LC and MLC are different but play both a relevant role in BBB diffusion of drugs.

## 2.4 P-GP AFFINITIES IN LOG BB PREDICTION

As already mentioned, each analyte present in the dataset was docked into each discrete binding site on the P-gp and the binding affinities were incorporated in the development of BBB passage predictive statistical models. Indeed, recent fuctional studies have identified seven sometimes overlapping binding sites accommodating substrates and inhibitors in the greasy, polyspecific binding cavity of P-gp. These binding sites were demonstrated able to allosterically communicate in a negative heterotropic manner. Moreover, an additional binding site was recognized on the exterior of P-gp bounded by residues from the transmembrane helices 9, 12 and the elbow helix 2. This site faces away from the transporter, lying close to the predicted membrane–water interface and intramembranous substrate-entry portal.

On average , highly clustered results were achieved, meaning that the conformational search procedure was exhaustive enough to ensure a coverage of the accessible conformational space. An extensive cluster analysis (RMSD tolerance was set to 2.0 Å) was performed and the binding affinity now reported in Table 2A and Table 2B are the minimum and the most populated binding energies of the clusters. The errors of the estimates of free energies of binding were never higher

297 than ± 1.8 kcal $mol^{-1}$. However, from the relationships reported above, P-gp affinities do not seem
298 to have an appreciable role in BBB passage. However, this is not entirely true because the statistical
299 model development was carried out using only four independent variables, thus leading the
300 software to select only the four most relevant descriptors, among which P-gp affinities were not
301 included. Indeed, when five independent variables were set in the statistical method development,
302 the P-gp binding affinities (Table 5A and 5B) were used by the software to build up the models.
303 Equations (21) and (22), generated by IAM indexes and four static properties of the analytes,
304 assumed as having zero atomic charges, is an example as can be seen in Table 5. The AutoDock
305 GPF/DPF files for site 1 and 7, i.e. the ones actually involved in the statistical models (21) and (22),
306 are now provided as supplementary materials.

307 This is not surprising because among the considered analytes, the only ones known from the
308 literature to be substrates of P-gp are cimetidine, domperidone, ranitidine, rifampicin, quinidine and
309 verapamil[26], and they represent less than 5% of the dataset. Indeed, the compounds considered were
310 selected in the attempt to mirror as accurately and completely as possible the marketed drugs, in
311 terms of diverse chemical nature, molecular volume, CNS activity and molecular lipophilicity.
312 Since the active transport comprises only for a minority of drugs, whereby the drug uptake in
313 mainly driven by passive transcellular diffusion, the limited predictivity of the P-gp molecular
314 affinity may be dataset related. This approach suffers from some limitations, the most evident one
315 being the aspect that the receptor flexibility is not taken into account. The main reason behind it is
316 the large number of degrees of freedom that should be considered in this kind of calculations, thus
317 requiring remarkable computational power. However, neglecting the receptor flexibility could lead
318 to poor docking results in terms of binding pose prediction in real-world settings. Therefore, these
319 results must be regarded as a preliminary attempt to gain new insights and model the active efflux
320 of drugs pumped out of cells by P-gp, being neither exhaustive nor complete. Other experiments
321 have to be performed and docking conditions further calibrated in order to validate the proposed

model.

**Table 5.** Statistical validation of the models developed employing either log $k_w^{SDS}$ or log $k_{30\%\ MeOH}^{IAM}$ values of the dataset (*n*=79) along with four (equations (29-32)) or five (equations (25-28)) other physico-chemical descriptors.

| STATIC | $r^2$ | $q^2$ | *SE* | *F* | *PC* | $r^2$ (n-1) | *SE* (n-1) | *F* (n-1) | *PC* (n-1) | EX-ROW | EQUATIONS | EQ No |
|---|---|---|---|---|---|---|---|---|---|---|---|---|
| MLC + IAM | 0.74 | 0.69 | 0.477 | 42.45 | 18.409 | 0.77 | 0.454 | 48.09 | 16.447 | - | log BB = -0.0521 + 0.5338 log $k_w^{SDS}$ + 0.3799 log $k_{30\%MeOH}^{IAM}$ - 0.0093 PSA - 0.0252 Dipole - 0.1057 VirtualLog P | 19 |
| | | | | | | | | | | Domperidone | log BB = -0.0506 + 0.5134 log $k_w^{SDS}$ + 0.4466 log $k_{30\%MeOH}^{IAM}$ - 0.0086 PSA - 0.0266 Dipole - 0.1120 VirtualLogP | 20 |
| P-GP AFFINITIES + IAM | 0.67 | 0.61 | 0.544 | 29.30 | 23.925 | 0.69 | 0.521 | 32.50 | 21.653 | - | log BB = 0.8837 + 0.9206 log k IAM - 0.0131 Psa - 0.2781 P-gp 1 Min - 0.1399 VirtualLogP + 0.2742 P-gp 7 MP | 21 |
| | | | | | | | | | | Celecoxib | log BB = 0.8118 + 0.9239 log $k_{30\%MeOH}^{IAM}$ - 0.0135 Psa - 0.1574 VirtualLogP - 0.2825 P-gp 1 Min + 0.2575 | 22 |

| | | | | | | | | | | | | |
|---|---|---|---|---|---|---|---|---|---|---|---|---|
| | | | | | | | | | | | P-gp 7 MP | |
| DRAGON DESCRIPTORS | | | | | | | | | | | | |
| MLC | 0.80 | 0.78 | 0.416 | 75.54 | 13.794 | 0.83 | 0.393 | 86.64 | 12.164 | - | log BB = -0.1663 + 0.6102 log $k_w^{SDS}$ - 0.0085 TPSA (NO) - 0.8563 nRCOOH - 0.0079 D/Dr05 | 23 |
| | | | | | | | | | | Verapamil | log BB = -0.2220 + 0.6483 log $k_w^{SDS}$ - 0.0078 TPSA (Tot) - 0.8677 nRCOOH - 0.0081 D/Dr05 | 24 |
| IAM | 0.76 | 0.73 | 0.457 | 59.13 | 16.711 | 0.78 | 0.440 | 65.45 | 15.242 | - | log BB = +0.4564 + 0.5250 log $k_{30\%\ MeOH}^{IAM}$ - 0.0091 TPSA (NO) -1.0354 nRCOOH – 0.0073 D/Dr05 | 25 |
| | | | | | | | | | | Verapamil | log BB = +0.4450 + 0.5490 log $k_{30\%\ MeOH}^{IAM}$ - 0.0086 TPSA (NO) – 1.0457 nRCOOH – 0.0082 D/Dr05 | 26 |

329
330
331

## 2.5 E-DRAGON DESCRIPTORS IN MAXIMIZING THE PREDICTIVE STRENGTH OF THE MODELS

In an attempt to further maximize the predictive strength of the models, IAM and MLC indexes were used in combination with E-Dragon descriptors[30]. The E-Dragon software calculates more than 1,600 descriptors, including not only the simplest atom type, functional group and fragment counts, but also several topological and geometrical descriptors. The results and statistical method validation are reported in Table 5. Remarkably high correlation coefficients were achieved with either IAM ($r^2$ = 0.78, equation (26)) or MLC ($r^2$= 0.83, equation (24)). As suggested by the similarly high $q^2$ values, those relationships are not affected by any over fitting. The plots of the experimental *vs* predicted log BB values (as predicted by equation (24)) are reported in Figure 3. Such relationship is based on MLC indexes, TPSA (Tot) i.e. the topological polar surface area using nitrogen, oxygen, sulphur, phosphorus polar contributions which differs from the TPSA (NO), included, for instance in equations (23), (25) and (26) that instead takes into account, in the topological polar surface area computation the nitrogen and oxygen contributions only. nRCOOH and D/Dr 05 are included in all the equations reported in Table 5. While the former is a functional group descriptor referring to the number of aliphatic carboxylic acids, the latter is a topological descriptor, named distance/detour ring index of order 5. It is based on operation over the distance/detour matrix D/Δ, a square symmetric matrix that contains the ratios of the lengths of the shortest to the longest path between any pair of vertices. It is calculated by the following equation:

$$\mathrm{D}/\Delta = \frac{1}{2}\sum_{i=l}^{A}\sum_{j=l}^{A}(D/\Delta)_{ij}$$

Although the role that such a parameter could play in the BBB partition is unclear, being its interpretation quite difficult, it cannot be excluded that it might affect the molecular flexibility of the analytes. However, the models obtained starting from E-Dragon descriptors would again support the view according to which the BBB penetration of drugs would be enhanced for highly

retained compounds either in IAM or MLC and hindered for compounds having greater PSA and supporting one or even more acidic functions. To further validate the proposed method, the datasets were divided randomly into 16 pairs of training and test sets. For each pair, the multiple linear regression was performed and the equations derived from the training sets were subsequently used to predict the log BB values of the test sets. Such value set was used to evaluate the regression coefficient ($r^2$), the standard error (SE) of the estimates and the Fischer coefficients. The results of this additional validation are shown in Table 6.

**Table 6.** Validation of the best model employing four descriptors for log BB prediction.

| Model Validation | | | | | |
|---|---|---|---|---|---|
| **Trial** | **Training set** | | | **Test set** | |
| | **$r^2$** | **SE** | **F** | **$r^2$** | **SE** |
| 1 | 0.87 | 0.320 | 57.459 | 0.75 | 0.496 |
| 2 | 0.85 | 0.412 | 46.645 | 0.71 | 0.445 |
| 3 | 0.84 | 0.411 | 45.880 | 0.71 | 0.498 |
| 4 | 0.84 | 0.390 | 45.696 | 0.74 | 0.488 |
| 5 | 0.84 | 0.415 | 43.969 | 0.75 | 0.433 |
| 6 | 0.84 | 0.394 | 43.432 | 0.75 | 0.450 |
| 7 | 0.83 | 0.389 | 41.407 | 0.77 | 0.455 |
| 8 | 0.81 | 0.427 | 35.093 | 0.76 | 0.445 |
| 9 | 0.80 | 0.444 | 35.085 | 0.78 | 0.411 |
| 10 | 0.80 | 0.438 | 34.173 | 0.77 | 0.430 |
| 11 | 0.80 | 0.426 | 33.984 | 0.79 | 0.453 |
| 12 | 0.80 | 0.482 | 33.303 | 0.79 | 0.372 |
| 13 | 0.80 | 0.444 | 33.181 | 0.78 | 0.424 |
| 14 | 0.79 | 0.444 | 32.284 | 0.79 | 0.413 |
| 15 | 0.77 | 0.462 | 28.660 | 0.81 | 0.404 |
| 16 | 0.75 | 0.476 | 25.656 | 0.82 | 0.393 |

.

**Figure 3**. Experimental *vs* Predicted log BB values plot for the best model obtained in the present study (Eq. (24)).

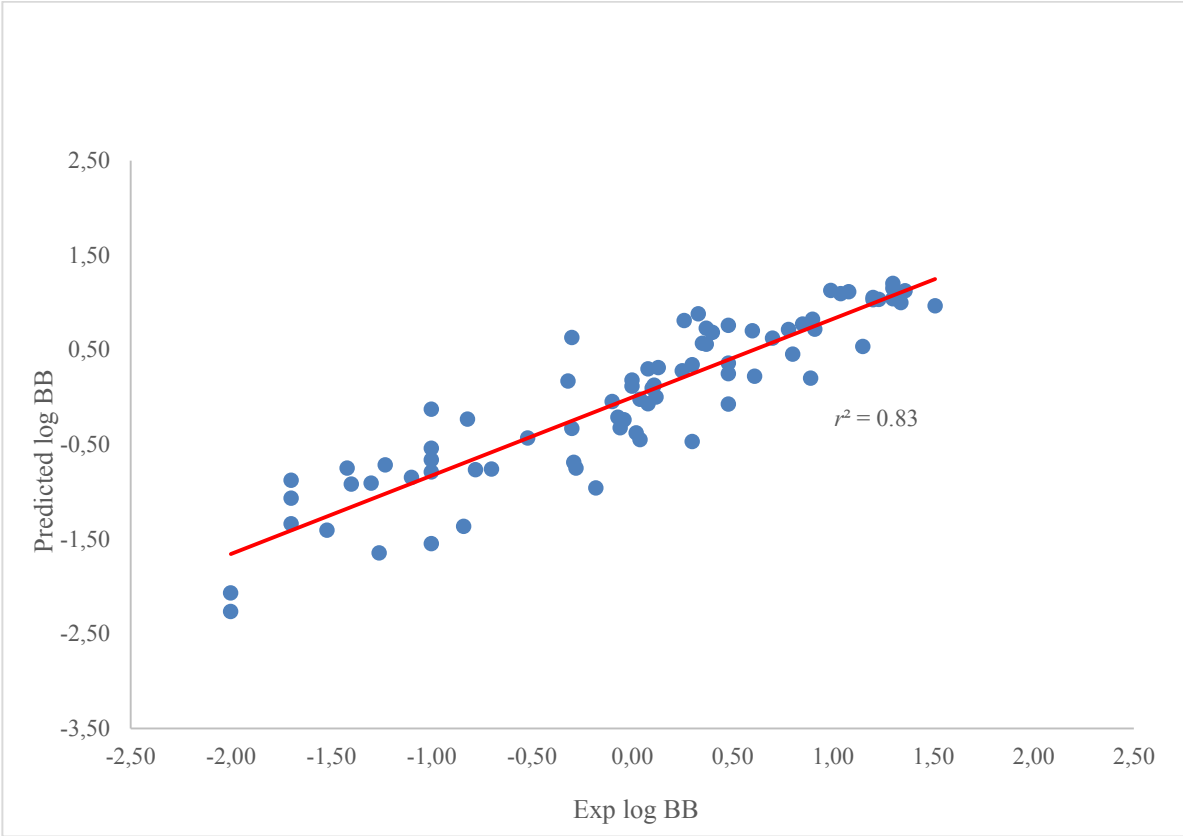

## 3.0 CONCLUSION

Highly significant ($r^2$ ($n$-1) up to 0.83) statistical methods for the BBB entering potential of drugs were achieved by applying the proposed method, which incidentally shed new light into BBB penetration of drugs. In fact, the BBB passage was found related to the analyte charges, being hindered for compounds supporting one or more acidic functions, and enhanced for bases. Moreover, molecules with higher dipolar momentum and greater PSA seemed less prone to cross the BBB. The relatively high number of analytes taken into account support statistically the suitability of the method as early screening method to evaluate BBB passage, and consolidate the novelty of the present work. In the modeling of drugs' BBB passage, both IAM and MLC indexes are found advantageously suitable; however, their combination with physico-chemical descriptors is highly beneficial for prediction. From a theoretical point of view, it should be considered that both IAM and MLC indexes relate to BBB passage data despite the different interactions they depict as confirmed by the lack of co-linearity between those two analytical indexes. Again, their simultaneous use in the statistic models, here performed for the first time, improved their prediction strength, thus suggesting that both play a relevant role in BBB passage although mirroring different phenomena. The P-gp efflux has also been investigated, but our results indicate that it would affect the overall BBB drug uptake only negligibly. However, this conclusion should be regarded cautiously due to the aspect that only a fewP-gp substrates were included in the set of analytes considered. Furthermore, the molecular docking simulations suffer from several limitations, the most important being the aspect that the receptor flexibility is not taken into account. This might have played a role in the moderate predictivity of the *in silico* calculated P-gp binding affinities. Finally, the proposed method is also suitable for pharmaceutical companies in the search for accurate BBB penetration oriented screening methods as the chromatographic conditions were carefully studied to obtain the indexes in a relatively short time such as to meet their demands. Chromatographic indexes (MLC and IAM) were always included in the best statistical models; this

404 implies that the information encoded in such measures is original and cannot be satisfactorily
405 surrogated by other *in silico* descriptors. The molecular modeling performed was simple, easy-to-
406 perform and can be configured to run automatically in case of batch analyses. Furthermore, as the
407 method is rather cheap and relies on basic HPLC equipment, it offers potential for broad scale
408 application

409 **4.0 EXPERIMENTAL SECTION**

410

411 4.1 CHEMICALS

412

413 The solutes were obtained from Sigma-Aldrich (Machelen, Belgium), TCI-Europe (Zwijndrecht,
414 Belgium) and Thermofisher Acros Organics (Geel, Belgium) as listed in Table 1 and their purity
415 was equal to or higher than 98%.

416
417 4.2 ANALYTICAL COLUMNS

418 MLC and IAM experiments were performed on an Agilent Zorbax SB-C18 Rapid Resolution (3.5
419 µm, 50 mm x 2.1 mm; Santa Clara, CA, USA) and Regis IAM Fast Mini Screening (10 µm, 10 mm
420 × 3.0 mm; Morton Grove, IL, USA) columns, respectively.

421 4.3 APPARATUS

422

423 4.3.1 MLC-HPLC

424 MLC chromatographic analysis was performed on an Alliance, Waters 2690 chromatograph
425 (Milford, MA, USA) with a quaternary pump and an automatic injector. A Waters 2487 dual-
426 wavelength absorbance ultraviolet detector was used. The applied detection wavelengths for the
427 various solutes were always in the range between 210 and 300 nm as listed in Table 1. Data

428 acquisition and processing were performed using a PeakSimple Chromatography Data System
429 (model 202) and PeakSimple software (SRI Instruments, Torrance, CA, USA). The temperature of
430 the analysis was controlled by a Polaratherm series 9000 unit (Selerity Technologies, Salt Lake
431 City, USA) and set at 37 °C. The flow rate was 1.0 mL $min^{-1}$ and the injection volume was 20 μL.

432 4.3.2. IAM-HPLC

433 IAM based chromatographic analysis was performed on an Agilent Capillary 1200 system (Santa
434 Clara, CA, USA). The system included a capillary pump, a micro vacuum degasser and an
435 automatic injector. An Agilent 1200 Series variable wavelength detector was used and set at the
436 maximum absorbance wavelength of each analyte. The IAM-HPLC experiments were carried out
437 at room temperature (20 ± 2 °C), the flow rate was 300 μL $min^{-1}$ and the injection volume was 1 μL.

438 4.4 MOBILE PHASE AND SAMPLE PREPARATION

439 MLC mobile phases were composed of aqueous solutions of 0.05 $mol \cdot L^{-1}$ sodium dodecyl sulfate
440 (SDS) (Acros). Water (18.2 $M\Omega \cdot cm^{-1}$) was purified and deionized in house via a Milli-Q plus
441 instrument from Millipore (Bedford, New Hampshire, USA). pH was adjusted to pH 7.4 by
442 phosphate buffer, prepared with 0.05 $mol \cdot L^{-1}$ disodium hydrogen phosphate (Sigma–Aldrich) and
443 potassium dihydrogen phosphate (Sigma–Aldrich). To reproduce the osmotic pressure of biological
444 fluids, NaCl (9.20 $g \cdot L^{-1}$) (Sigma–Aldrich) was added to the micellar mobile phase. IAM mobile
445 phases consisted of a solution 70/30 v/v Dulbecco's phosphate-buffered saline (DPBS) / methanol
446 (HPLC-grade; Biosolve, Valkenswaard, The Netherlands). DPBS was composed of 2.7 $mmol \cdot L^{-1}$
447 KCl, 1.5 $mmol \cdot L^{-1}$ potassium dihydrogen phosphate, 137.0 $mmol \cdot L^{-1}$ NaCl, and 8.1 $mmol \cdot L^{-1}$
448 disodium hydrogen phosphate (Sigma–Aldrich). Such solution had a pH value of 7.40 ± 0.05, and
449 no pH adjustment was performed. All mobile phases were vacuum-filtered through 0.20 μm nylon
450 membranes (Grace, Lokeren, Belgium) before use. Different mobile phases and elution programs
451 were tested starting from 100% aqueous phase; however, in IAM-LC the latter condition did not
452 allow the elution of the most lipophilic bases in a reasonable amount of time. Stock solutions of all

453 drugs were prepared by dissolving 10 mg in 1 mL of methanol except for i) quinidine and
454 theobromine, for which stock concentrations of 1 $mg \cdot mL^{-1}$ and 200 $\mu g \cdot mL^{-1}$, respectively, were
455 used, ii) caffeine and theophylline, which were dissolved in water (10 $mg \cdot mL^{-1}$), iii) domperidone,
456 which was dissolved in dimethyl sulfoxide (10 $mg \cdot mL^{-1}$) and iv) chlorpromazine, which was
457 dissolved in acetonitrile. Stock solutions were stored at 4 °C, except for atenolol, zidovudine,
458 chlorambucil and rifampicin, which were stored at −20 °C. Working solutions were freshly
459 prepared at the beginning of each day by dilution, with the mobile phase, of the stock solutions to
460 50 $\mu g \cdot mL^{-1}$ for all the analytes, except for valproic acid and halothane that were diluted to 250
461 $\mu g \cdot mL^{-1}$.

462 4.5 DATA SOURCES

463 Log BB values were taken from the literature[18–24]. pKa values were obtained from the literature[21]
464 except for amobarbital, donepezil, fluphenazine, hydroxyzine, ketorolac, paroxetine and ropinirole,
465 whose values were calculated by the software Marvin Sketch 15.1 for Mac OS X[28].

466 4.6 SOFTWARE

467

468 4.6.1 MOLECULAR MODELING

469 Molecular modeling was performed by the software Vega ZZ 3.0.5 for Windows-based PCs[31]. The
470 starting three-dimensional structures of the considered molecules were downloaded from PubChem
471 database[32] and they were considered in both zero atomic charge and ionized form. The Gasteiger –
472 Marsili[33] method, along with CHARMM[34,35,36] force field, was applied to calculate the atomic
473 charges required to perform the next molecular mechanics calculations. An extensive
474 conformational analysis was carried out *in vacuum* by using the Boltzmann Jump method
475 (MonteCarlo procedure) implemented in AMMP software[37] which generates 1000 geometries for
476 each compound by randomly rotating the rotors and the obtained lowest energy conformation was
477 further optimized by performing a PM7 semi-empirical calculation with MOPAC 2012 program[38]

478 (keywords: PM7 PRECISE MMOK). A cluster analysis was performed to select the most populated
479 conformation states. Physico-chemical and topological/geometrical properties (Virtual logP[39],
480 lipole[40], volume, polar surface area, surface accessible to the solvent, gyration radius, ovality, mass,
481 number of atoms, angles, dihedrals, etc) were calculated by VEGA ZZ software and, finally, all
482 molecules were inserted into a Microsoft Access database.
483 The QSPR models were obtained by the automatic stepwise approach implemented in "Automatic
484 linear regression" script of VEGA ZZ software, calculating regression models, including from 1 to
485 5 independent variables. The predictive strength of the best equation was evaluated by leave-one-
486 out (LOO) cross validation and the regression coefficients were calculated to evaluate the set in
487 terms of standard deviation of errors, angular coefficient, intercept and $r^2$ of the trend line of the
488 chart of the predicted *vs.* experimental activities. Descriptors with too low regression coefficient ($r^2$
489 $< 0.1$) were excluded and collinear descriptors were detected by evaluating the variance inflation
490 factor (VIF) whose threshold value was set to 5. A further validation of the model having the
491 highest predictive strength was performed *via* model validator script, included in Vega.
492
493 4.6.2 MOLECULAR DOCKING
494 Molecular docking calculations were carried out using AutoDock 4.2 software[41]. The 3.4 Å
495 resolution P-glycoprotein (P-gp) crystallographic structure (mouse P-glycoprotein 3, gene: MD1A,
496 PDB code: 4Q9H) was downloaded from Protein Data Bank (PDB) Database. Gasteiger partial
497 charges were calculated on ligand atoms. Polar hydrogens were added to P-gp and Gesteiger[33]
498 partial charges were calculated using AutoDock Tools[42]. Simulation boxes were centered on the
499 ligands in the structures of P-gp-ligand complexes (PDB codes: 4Q9I, 4Q9J, 4Q9K, 4Q9L) as
500 reported in the literature[27]. The simulation boxes were adjusted to accommodate the ligand in each
501 complex and the sizes were between 26x26x26 Å and 30x26x30 Å. 100 runs for each simulation
502 were performed and the Lamarckian Genetic Algorithm (number of energy evaluation: $2.5 \times 10^6$)
503 for the docking simulations was used. The choice was based on the aspect that this protocol

504 provides the most efficient search for general applications, and is typically effective for systems
505 with about 10 rotatable bonds in the ligand. The acidic compounds having pKa < 7.4 and the basic
506 ones having pKa > 7.4 were considered in their dissociated forms. Gasteiger-Marsili[33] electric
507 charges were supplied. Amphoteric drugs were assumed in their prevalent forms as calculated by
508 the software MarvinSketch[28]. For the analytes supporting one or more stereocenters, the following
509 arrangements were undertaken. When the drugs were administered as racemic mixture (Atenolol,
510 Citalopram, Donepezil, Eserine, Halothane, Hexobarbital, Hydroxyzine, Ibuprofen, Ketorolac,
511 Mianserin, Nicotine, Omeprazole, Oxazepam, Pindolol, Promethazine, Venlafaxine and
512 Verapamil), each stereoisomer was docked into each site of the P-gp and the binding energies
513 presented are the averages of those of the stereoisomers included in the mixtures. On the contrary,
514 when the log BB values referred to a specific stereoisomer (Rifampicine, Zidovudine,
515 Levofloxacin) as that was the one administered in the log BB determinations, only this was docked.
516 When a new stereocenter was created because of protonation, as for instance occurs for tertiary
517 amines supporting different groups, both configurations were tested. The consistency of the results
518 was analyzed by clustering spatially the docked conformations. This step was necessary because of
519 the stochastic nature of the search methods, that are used to predict optimal docked conformations.

520 4.7 PROCESSING

521 The chromatographic retention coefficients of each analytes were calculated by using the following
522 expression:

523 $$k = \frac{t_r - t_0}{t_0}$$

524 in which $t_r$ is the retention time of the compound of interest and $t_0$ the retention time of a non-
525 retained compound (acetone). All reported log k values are the average of at least three
526 measurements; for each log k value the 95% confidence interval associated with each value never

527 exceeded 0.04.

528 Three different sets of properties were generated. At first, all the analytes were considered as
529 uncharged (having full charge equal to 0), subsequently analytes having acidic or basic functions
530 were considered fully ionized and zwitterions were considered with both the acidic and basic
531 functions in their charged forms. Eventually, a weighted average of the static properties at pH 7.4
532 according to the pKa of each analyte was performed; for zwitterions, the relative abundance of each
533 microspecies (zero atomic charges, zwitterion, anion and cation) in solution at the physiological pH
534 (7.4) was calculated by the software Marvin Sketch 15.1 for Mac OS X[28]. This approach was also
535 extended to the conformational analysis performed *in vacuum*, yielding three different sets of
536 conformational properties, i.e. i) conformational properties of the forms of the analytes having zero
537 atomic charges, ii) conformational properties of the ionized forms of the analytes, and iii) average
538 of the conformational properties at pH 7.4 according to the pKa of each analyte and the calculated
539 microspecies distribution for zwitterions. For each of the properties taken into account (Molecular
540 lipophilicity potential (MLP)[39], lipole[40], volume, polar surface area, superficial area, gyration
541 radius, ovality, volume diameter, dipolar moment, etc), minimum and maximum value, average,
542 range and standard deviation for each population of conformers were calculated and incorporated in
543 the statistical models. An additional deal of molecular descriptor were calculated by the software E-
544 Dragon[30].

545 **Conflict of interest disclosure**

546 The authors declare no competing financial interest.

547

548 **LIST OF ABBREVIATIONS**

549

550 *CNS* Central Nervous System; *D/Dr05* distance/detour ring index of order 5; *Impropers* Number of
551 improper angles (out of plane); *HbDon* Number of H-bond donor groups; *HbAcc* Number of H-

552 bond acceptor groups; *IAM* Immobilized artificial membrane; *MD* Dipole Moment (Debye); *MLC*
553 Micellar liquid chromatography; *MLP* Molecular Lipophilicity Potential; *nRCOOH* number of
554 carboxylic group (aliphatic); *PLS* Partial Least Squares; *Psa* Polar Surface Area ($Å^2$); *P-gp* P-
555 glycoprotein; *SDS* sodium dodecyl sulphate; *TPSA (NO)* topological polar surface area using N,O
556 polar contributions; *TPSA (Tot)* topological polar surface area using N,O,S,P polar contributions.
557

**Supporting Information**

- Figure 1 Page S-2;
- Figure 2 Page S-4;
- Figure 3 Page S-6;
- raw data in the spreadsheet file “data.xlsx”.
- AutoDock GPF file for site 1
- AutoDock DPF file for site 1
- AutoDock GPF file for site 7
- AutoDock DPF file for site 7

To whom correspondence should be addressed:

Prof. Dr. Frederic Lynen

Separation Science Group

Department of Organic and Macromolecular Chemistry

Ghent University

Krijgslaan 281, S4-bis

B-9000 Gent, Belgium

Tel. +(32)9 264 96 02

Fax +(32)9 264 49 98

e-mail: frederic.lynen@ugent.be

-

583 **5.0 REFERENCES**


584 (1) Waring, M.J.; Arrowsmith, J.; Leach, A.R.; Leeson, P.D.; Mandrell, S.; Owen, R.M.;
585 Pairaudeau, G.; Pennie, W.D.; Pickett, S.D.; Wang, J.; Wallace, O.; Weir, A. An Analysis of
586 the Attrition of Drug Candidates from Four Major Pharmaceutical Companies. *Nat. Rev.*
587 *Drug Discov.* **2015**, *14* (7), 475–486.

588 (2) Kola, I.; Landis, J. Can the Pharmaceutical Industry Reduce Attrition Rates? *Nat. Rev. Drug*
589 *Discov.* **2004**, *3* (August), 1–5.

590 (3) Van Bree, J. B.; De Boer, A. G.; Danhof, M.; Breimer, D. D. Drug Transport across the
591 Blood--Brain Barrier. I. Anatomical and Physiological Aspects. *Pharm. Weekbl. Sci. Ed.*
592 **1992**, *14* (5), 305–310.

593 (4) Keaney, J.; Campbell, M. The Dynamic Blood-Brain Barrier. *FEBS J.* **2015**, *282* (21), 4067–
594 4079.

595 (5) Bickel, U. How to Measure Drug Transport across the Blood-Brain Barrier. *NeuroRx* **2005**, *2*
596 (1), 15–26.

597 (6) Lundquist, S.; Renftel, M.; Brillault, J.; Fenart, L.; Cecchelli, R.; Dehouck, M.-P. Prediction
598 of Drug Transport through the Blood-Brain Barrier in Vivo: A Comparison between Two in
599 Vitro Cell Models. *Pharm. Res.* **2002**, *19* (7), 976–981.

600 (7) Ekins, S.; Mestres, J.; Testa, B. In Silico Pharmacology for Drug Discovery: Applications to
601 Targets and Beyond. *Br. J. Pharmacol.* **2007**, *152* (December 2006), 21–37.

602 (8) Grumetto, L.; Russo, G.; Barbato, F. Indexes of Polar Interactions between Ionizable Drugs
603 and Membrane Phospholipids Measured by IAM-HPLC: Their Relationships with Data of
604 Blood-Brain Barrier Passage. *Eur. J. Pharm. Sci.* **2014**, *65*, 139–146.

605 (9) De Vrieze, M.; Verzele, D.; Szucs, R.; Sandra, P.; Lynen, F. Evaluation of Sphingomyelin,
606 Cholester, and Phosphatidylcholine-Based Immobilized Artificial Membrane Liquid
607 Chromatography to Predict Drug Penetration across the Blood-Brain Barrier. *Anal. Bioanal.*

608 *Chem.* **2014**, *406* (25), 6179–6188.

609 (10) Barbato, F.; Di Martino, G.; Grumetto, L.; La Rotonda, M. I. Prediction of Drug-Membrane
610 Interactions by IAM-HPLC: Effects of Different Phospholipid Stationary Phases on the
611 Partition of Bases. *Eur. J. Pharm. Sci.* **2004**, *22* (4), 261–269.

612 (11) Grumetto, L.; Russo, G.; Barbato, F. Relationships between Human Intestinal Absorption
613 and Polar Interactions Drug/phospholipids Estimated by IAM-HPLC. *Int. J. Pharm.* **2015**,
614 *489* (1–2), 186–194.

615 (12) Grumetto, L.; Russo, G.; Barbato, F. Immobilized Artificial Membrane HPLC Derived
616 Parameters vs PAMPA-BBB Data in Estimating in Situ Measured Blood–Brain Barrier
617 Permeation of Drugs. *Mol. Pharm.* **2016**, *13(8),* 2808-2816.

618 (13) Grumetto, L.; Russo, G.; Barbato, F. Polar Interactions Drug/phospholipids Estimated by
619 IAM-HPLC vs Cultured Cell Line Passage Data: Their Relationships and Comparison of
620 Their Effectiveness in Predicting Drug Human Intestinal Absorption. *Int. J. Pharm.* **2016**,
621 *500* (1–2), 275–290.

622 (14) De Vrieze, M.; Janssens, P.; Szucs, R.; Van der Eycken, J.; Lynen, F. In Vitro Prediction of
623 Human Intestinal Absorption and Blood-Brain Barrier Partitioning: Development of a Lipid
624 Analog for Micellar Liquid Chromatography. *Anal. Bioanal. Chem.* **2015**, *407* (24), 7453–
625 7466.

626 (15) Verzele, D.; Lynen, F.; Vrieze, M. D.; Wright, A. G.; Hanna-Brown, M.; Sandra, P.
627 Development of the First Sphingomyelin Biomimetic Stationary Phase for Immobilized
628 Artificial Membrane (IAM) Chromatography. *Chem. Commun.* **2012**, *48* (8), 1162–1164.

629 (16) De Vrieze, M.; Lynen, F.; Chen, K.; Szucs, R.; Sandra, P. Predicting Drug Penetration across
630 the Blood-Brain Barrier: Comparison of Micellar Liquid Chromatography and Immobilized
631 Artificial Membrane Liquid Chromatography. *Anal. Bioanal. Chem.* **2013**, *405*, 6029–6041.

632 (17) Berthod, A.; Garcia-Alvarez-Coque, C. Micellar Liquid Chromatography; Marcel Dekker
633 Incorporated, New York, 2000.

634 (18) Abraham, M. H.; Chadha, H. S.; Whiting, G. S.; Mitchell, R. C. Hydrogen Bonding. 32. An
635 Analysis of Water-Octanol and Water-Alkane Partitioning and the Deltalog P Parameter of
636 Seiler. *J. Pharm. Sci.* **1994**, *83* (8), 1085–1100.
637 (19) Katritzky, A. R.; Kuanar, M.; Slavov, S.; Dobchev, D. A.; Fara, D. C.; Karelson, M.; Acree,
638 W. E.; Solov'ev, V. P.; Varnek, A. Correlation of Blood-Brain Penetration Using Structural
639 Descriptors. *Bioorganic Med. Chem.* **2006**, *14* (14), 4888–4917.
640 (20) Platts, J. A.; Abraham, M. H.; Zhao, Y. H.; Hersey, A.; Ijaz, L.; Butina, D. Correlation and
641 Prediction of a Large Blood-Brain Distribution Data Set - An LFER Study. *Eur. J. Med.*
642 *Chem.* **2001**, *36* (9), 719–730.
643 (21) Avdeef, A. Absorption and Drug Development; John Wiley & Sons, Inc.: Hoboken, NJ,
644 USA, 2012; pp 625–663.
645 (22) Mente, S. R.; Lombardo, F. A Recursive-Partitioning Model for Blood-Brain Barrier
646 Permeation. *J. Comput. Aided. Mol. Des.* **2005**, *19* (7), 465–481.
647 (23) Abraham, M. H.; Ibrahim, A.; Zhao, Y.; Jr, W. E. A.; Al, A. E. T. A Data Base for Partition
648 of Volatile Organic Compounds and Drugs From Blood / Plasma / Serum to Brain , and an
649 LFER Analysis of the Data. *J. Pharm. Sci.* **2006**, *95* (10), 2091–2100.
650 (24) Björkman, S. Prediction of the Volume of Distribution of a Drug: Which Tissue-Plasma
651 Partition Coefficients Are Needed? *J. Pharm. Pharmacol.* **2002**, *54* (9), 1237–1245.
652 (25) Avdeef, A. Absorption and Drug Development; John Wiley & Sons, Inc.: Hoboken, NJ,
653 USA, 2012; p 595–602 and references cited therein.
654 (26) Eyal, S.; Hsiao, P.; Unadkat, J. D. Drug Interactions at the Blood-Brain Barrier: Fact or
655 Fantasy? *Pharmacol. Ther.* **2009**, *123* (1), 80–104.
656 (27) Szewczyk, P.; Tao, H.; McGrath, A. P.; Villaluz, M.; Rees, S. D.; Lee, S. C.; Doshi, R.;
657 Urbatsch, I. L.; Zhang, Q.; Chang, G. Snapshots of Ligand Entry, Malleable Binding and
658 Induced Helical Movement in P-Glycoprotein. *Acta Crystallogr. Sect. D Biol. Crystallogr.*
659 **2015**, *71*, 732–741.

660 (28) ChemAxon. Marvin Sketch.
661 (29) Vistoli, G.; Pedretti, A.; Testa, B. Partition Coefficient and Molecular Flexibility: The
662 Concept of Lipophilicity Space. *Chem. Biodivers.* **2009**, *6* (8), 1152–1169.
663 (30) Tetko, I. V; Gasteiger, J.; Todeschini, R.; Mauri, A.; Livingstone, D.; Ertl, P.; Palyulin, V.
664 A.; Radchenko, E. V; Zefirov, N. S.; Makarenko, A. S.; Tanchuk, V. Y.; Prokopenko, V. V.
665 Virtual Computational Chemistry Laboratory--Design and Description. *J. Comput. Aided.*
666 *Mol. Des.* **2005**, *19* (6), 453–463.
667 (31) Pedretti, A.; Villa, L.; Vistoli, G. VEGA - An Open Platform to Develop Chemo-Bio-
668 Informatics Applications, Using Plug-in Architecture and Script Programming. *J. Comput.*
669 *Aided. Mol. Des.* **2004**, *18* (3), 167–173.
670 (32) Kim, S.; Thiessen, P. A.; Bolton, E. E.; Chen, J.; Fu, G.; Gindulyte, A.; Han, L.; He, J.; He,
671 S.; Shoemaker, B. A.; Wang, J.; Yu, B.; Zhang, J.; Bryant, S. H. PubChem Substance and
672 Compound Databases. *Nucleic Acids Res.* **2016**, *44* (D1), D1202-1213.
673 (33) Gasteiger, J.; Marsili, M. Iterative Partial Equalization of Orbital Electronegativity-a Rapid
674 Access to Atomic Charges. *Tetrahedron* **1980**, *36* (22), 3219–3228.
675 (34) Brooks, B. R.; Brooks, C. L., 3rd; Mackerell, A. D., Jr.; Nilsson, L.; Petrella, R. J.; Roux, B.;
676 Won, Y.; Archontis, G.; Bartels, C.; Boresch, S.; Caflisch, A.; Caves, L.; Cui, Q.; Dinner, A.
677 R.; Feig, M.; Fischer, S.; Gao, J.; Hodoscek, M.; Im, W.; Kuczera, K.; Lazaridis, T.; Ma, J.;
678 Ovchinnikov, V.; Paci, E.; Pastor, R. W.; Post, C. B.; Pu, J. Z.; Schaefer, M.; Tidor, B.;
679 Venable, R. M.; Woodcock, H. L.; Wu, X.; Yang, W.; York, D. M.; Karplus, M. CHARMM:
680 the biomolecular simulation program. *J. Comput. Chem.* **2009**, *30*, 1545-1614.
681 (35) Brooks, B. R.; Bruccoleri, R. E.; Olafson, B. D.; States, D. J.; Swaminathan, S.; Karplus, M.
682 CHARMM: A program for macromolecular energy, minimization, and dynamics
683 calculations. *J. Comput. Chem.* **1983**, *4*, 187-217.
684 (36) MacKerell, A. D.; Brooks, B.; Brooks, C. L.; Nilsson, L.; Roux, B.; Won, Y.; Karplus, M.
685 CHARMM: The Energy Function and Its Parameterization with an Overview of the Program.

686 In *Encyclopedia of Computational Chemistry*, 1st ed.; Schleyer, P. v. R., Ed.; John Wiley &
687 Sons, Inc.: Chichester, UK, **1998;** 271-277.
688
689 (37) Harrison, R. W. Stiffness and Energy-Conservation Molecular-Dynamics - An Improved
690 Integrator. *J. Comput. Chem.* **1993**, *14* (9), 1112–1122.
691 (38) Stewart, J. J. P. MOPAC: A Semiempirical Molecular Orbital Program. *J. Comput. Aided.*
692 *Mol. Des.* **1990**, *4* (1), 1–103.
693 (39) Gaillard, P.; Carrupt, P. A.; Testa, B.; Boudon, A. Molecular Lipophilicity Potential, a Tool
694 in 3D QSAR: Method and Applications. *J. Comput. Aided. Mol. Des.* **1994**, *8* (2), 83–96.
695 (40) Pedretti, A.; Villa, L.; Vistoli, G. Modeling of Binding Modes and Inhibition Mechanism of
696 Some Natural Ligands of Farnesyl Transferase Using Molecular Docking. *J. Med. Chem.*
697 **2002**, *45* (7), 1460–1465.
698 (41) Huey, R.; Morris, G. M.; Olson, A. J.; Goodsell, D. S. Software News and Update. A
699 Semiempirical Free Energy Force Field with Charge-Based Desolvation. *J. Comput. Chem.*
700 **2007**, *28*, 1145–1152.
701 (42) Morris, G. M.; Ruth, H.; Lindstrom, W.; Sanner, M. F.; Belew, R. K.; Goodsell, D. S.;
702 Olson, A. J. Software News and Updates AutoDock4 and AutoDockTools4: Automated
703 Docking with Selective Receptor Flexibility. *J. Comput. Chem.* **2009**, *30* (16), 2785–2791.
704
705
706
707
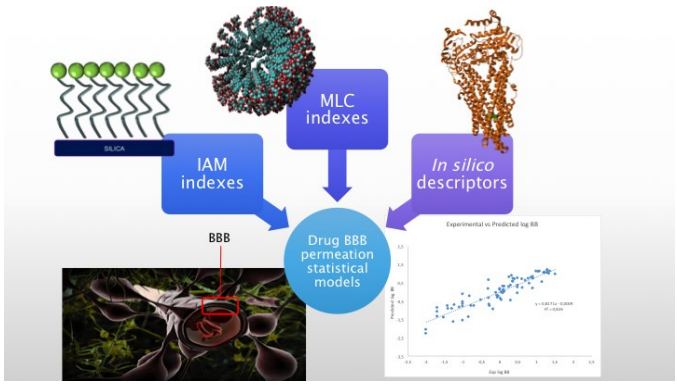
**TABLE OF CONTENTS GRAPHIC**